Lympholyte-M (Cedarlane, Hornby, ON, Canada), and serially fractionated with immunomicrobeads and AutoMACS (Miltenyi Biotech, Bergisch Gradbach, Germany). Lineage-negative (Lin^-) and –positive (Lin^+) cells were separated with a Lineage Cell Depletion Kit (Miltenyi Biotech). Sca1-, CD45R (B220)- and CD90 (Thy1.2)-positive cells ($Sca1^+$, $B220^+$ and $Thy1.2^+$ cells, respectively) were separated with appropriate microbeads (Miltenyi Biotech). Lin^-Sca1^+ cells were used as HSCs. Lin^+B220^+ cells and $Lin^+Thy1.2^+$ cells were used as B-lymphocytes and T-lymphocytes, respectively.

Coculture of HSCs and stromal cells

10T1/2, A54 and M1601 stromal cells were inoculated (5 x 10^3 cells/well) on a 12-well culture plate (Falcon 3043, BD, Franklin Lakes, NJ, USA). After 2 days, the near-confluent cells (ca. 2 x 10^4 cells/well) were gamma-irradiated (30 Gy) using a Gammacell 40 Exactor (Nordion International, Ottawa, ON, Canada) to prevent hyperproliferation. Then 1 x 10^4 HSCs (Lin^-Sca1^+ cells) were added to the irradiated stromal cells and cocultured for 5 days in α-Minimum Essential Medium (Invitrogen) supplemented with 10% FBS. A coculture was also carried out using a Cell Culture Insert (Falcon 353090, BD) on a 6-well culture plate (Falcon 3046, BD) for 5 days, with HSCs seeded in the upper wells and stromal cells in the lower wells. After coculture, cells were examined for cobblestone formation (30 or more clustered HSCs) on an inverted fluorescent microscope (Olympus IX-70, Tokyo, Japan), and the stromal cells and HSCs were separated with MACSelect K^k microbeads (Miltenyi Biotech) and AutoMACS for further analyses. The stromal cells derived from C3H mouse ($H\text{-}2^k$) were separated as a positive fraction, and HSCs derived from C57BL/6 mouse ($H\text{-}2^b$) were separated as a negative fraction. The separated cells were stained with a phycoerythrin-conjugated anti-mouse $H\text{-}2K^k$ antibody and a fluorescein isothiocyanate-conjugated anti-mouse $H\text{-}2K^b$ antibody (BD Biosciences, San Jose, CA, USA), and the purity was evaluated with BD LSR and CellQuest software (BD Immunosystems, Mountain View, CA, USA). For colony asaay after coculture, separated HSCs were cultivated (1 x 10^3 cells/35 mm dish) in growth factor-containing methylcellulose medium (MethoCult GF M3434, StemCell Technologies, Vancouver, BC, Canada) and colonies were counted on day 7.

Gene expression analysis

To quantify several signaling molecules, the reverse transcriptase-directed polymerase chain reaction (RT-PCR) was performed. Total RNA was extracted from the cells using an RNeasy Mini Kit (QIAGEN, Hilden, Germany), and cDNA was synthesized with a SuperScript First-Strand Synthesis Kit (Invitrogen). PCR was carried out with a QuantiTect SYBR Green PCR Kit (QIAGEN), and the incorporation of the fluorescent dye into the PCR products was monitored with ABI Prism 7700 (Applied Biosystems, Foster City, CA, USA). As internal controls, beta-actin was used for the stromal cells and glyceraldehyde-3-phosphate dehydrogenase was used for HSCs. The primers for PCR are listed in Table 1. Gene expression profiles of A54 before and after coculture with HSCs were compared using a FilgenArray Mouse 32K (Filgen, Nagoya, Japan).

Table 1. RT-PCR primer design.

Target	Forward primer	Reverse primer
Ang1	CCAATCTAAATGGAATGTTCT	CAGAGCACCTTCAAAAGTCCA
beta-actin	CCATCATGAAGTGTGACGTTG	GTCCGCCTAGAAGCACTTGCG
BMP6	TTCTCCCCACATCAACGACACC	AAACTCCCCACCACACAGTCC
Dll3	CCAGTAGCTGCCTGAACTCC	ATTGAAGCAGGGTCCATCTG
GAPDH	CCTGGAGAAACCTGCCAAGTATG	AGAGTGGGAGTTGCTGTTGAAGTC
Hes1	AAAGCCTATCATGGAGAAGAGGCG	GGAATGCCGGGAGCTATCTTTCTT
Jag1	CCGTAATCGCATCGTACTGC	GGCCTCCACCAGCAAAGTGT
Notch1	TGTTAATGAGTGCATCTCCAACCCA	CATTCGTAGCCATCAATCTTGTCC
SCF	ATGGACAGCCATGGCATTGC	CACCTCTTGAAATTCTCTCT
SDF1	GCCCTTCAGATTGTTGCA	CGTCTGACTCACACCTCACA

Immunostaining

A54 cells and HSCs were cocultured on Culture Slides (Falcon 354111, BD), and immunostained on day 5. The cells were fixed with 4% paraformaldehyde, and incubated with a rabbit anti-mouse Jag1 antibody (ab7771, Abcam, Cambridge, UK) and Alexa Fluor 488-conjugated goat anti-rabbit IgG (A11008, Invitrogen) for 30 minutes on ice, respectively. Slides were inspected and photographed under an IX-70 microscope.

Statistical analysis

The statistical analysis was performed using a Statcel2 (OMS Publishing, Saitama, Japan) add-on package for Microsoft Excel. Student's t-test was used for comparison between two groups, and a multiple comparison test (the Turkey-Kramer method) was used for comparison among groups of three or more. A P-value < 0.05 was considered to be significant for all analyses.

Results

Requirement of cell contact in supporting hematopoeisis

In coculure experiments with 10T1/2 or its derivatives (A54 and M1601), HSCs formed cobblestone areas only on A54 at day 5 (12.5 ± 0.6 cobblestone areas/10^4 cells), as we reported previously [14]. We also confirmed that the murine hematopoietic progenitors were expanded by ninefold (36.0 ± 4.0 colonies/10^3 cells post-coculture with A54 vs. 4.0 ± 2.0 colonies/10^3 cells pre-coculture, Figure 1) whereas the number of hematopoietic progenitors was not significantly increased after the coculture with parental 10T1/2 cells or M1601 myoblasts (3.3 ± 1.5 colonies/10^3 cells with 10T1/2, and 6.3 ± 1.5 colonies/10^3 cells with M1601; Figure 1). Without stromal cell support, HSCs completely lost their progenitor activity in the same medium used for coculture ('No stroma' in Figure 1). Indeed, only few monocyte/macrophage-like cells were found after 5-day-incubation in this population; we speculated that all the clonogenic cells fell into apoptosis because no additional cytokine was provided. As we previously reported, expression of SCF, SDF1 and Ang1 in A54 was greater than that in 10T1/2 and M1601cells [14]. Such an overexpression of SCF, SDF1 and Ang1 in A54 cells was not further augmented or cancelled by addition of interleukin-1 or coculture with HSCs (data not shown).

Next, we addressed whether soluble factors from A54 preadipocytes were sufficient for supporting hematopoiesis. To discriminate the contribution of cell communication via direct adhesion, mouse bone marrow-derived HSCs were cultivated on a microporous membrane (1 micron Cell Culture Insert) placed in a well containing A54 cells underneath. We found that physical separation from A54 cells totally abrogated the progenitor activity of HSCs, in spite of the availability of soluble molecules from the stromal cells (Figure 1). This observation indicated that A54 cells supported hematopoiesis by cell contact in addition to secreting cytokines.

Gene expression changes in preadipocytes cocultured with HSCs

Upon learning that cell adhesion is required for A54 cells to support HSCs, we speculated that some signaling from HSCs to stromal cells might occur during coculture. This idea prompted us to search for molecules whose expression changed in A54 cells cocultured with HSCs. Total RNA was extracted from A54 cells before and after the coculture and gene expression profiles were compared by microarray. Out of 33696 genes screened, 353 genes were upregulated by twofold or more after the coculture with HSCs, and 13 genes were downregulated to the levels less than a half of starting value (data not shown). Among them, 29 genes (21 upregulated and 8 downregulated; Table 2) were implicated to be involved in hematopoiesis. Therefore we focused on these molecules for further investigation. A quantitative RT-PCR analysis confirmed the upregulation of Jagged 1 (Jag1), Delta-like 3 (Dll3) and bone morphogenetic protein 6 (BMP6) in A54 cells after coculture with HSCs (Figure 2). On the other hand, upregulation of Jag1, Dll3 and BMP6 was not observed in the undifferentiated 10T1/2 cells or M1601 myoblasts after coculture with HSCs (data not shown). Expression of Jag1 was also increased in A54 cells cultured with differentiated cells such as B- and T-lymphocytes, but to a lesser extent (Figure 2A).

Figure 1

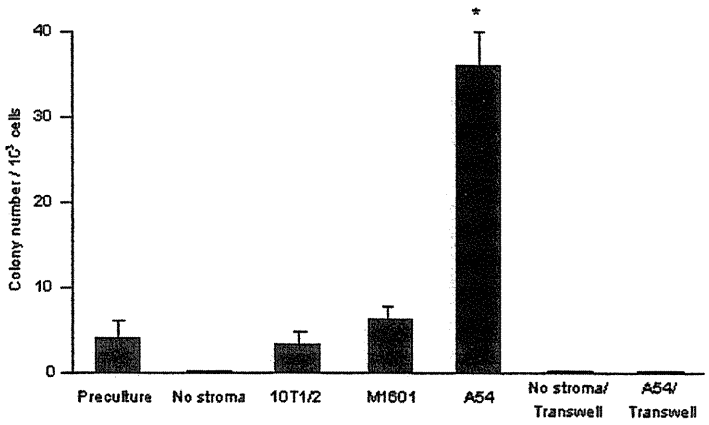

Figure 1. Requirement of direct contact for preadipocytes to support hematopoiesis. 1 x 10^4 mouse bone marrow Lin^-Sca1^+ cells (HSCs) were cocultured with 2 x 10^4 C3H10T1/2 cells (10T1/2), 10T1/2-derived myoblasts (M1602) or preadipocytes (A54) for 5 days. After coculture, HSCs were separated with immunomagnetic beads and subjected to colony assay. HSCs were seeded on MethoCult GF M3434 (1 x 10^3 cells/dish) and colonies were counted on day 7. Preculture: colonies from HSCs prior to coculture. No stroma: colonies from HSCs incubated 5 days without stromal support. No stroma/Transwell: colonies from HSCs seeded on the top wells, with no stromal cells in the bottom wells. A54/Transwell: HSCs were coincubated with A54 but separated by Cell Culture Insert. *: P < 0.01 (n = 3).

Figure 2

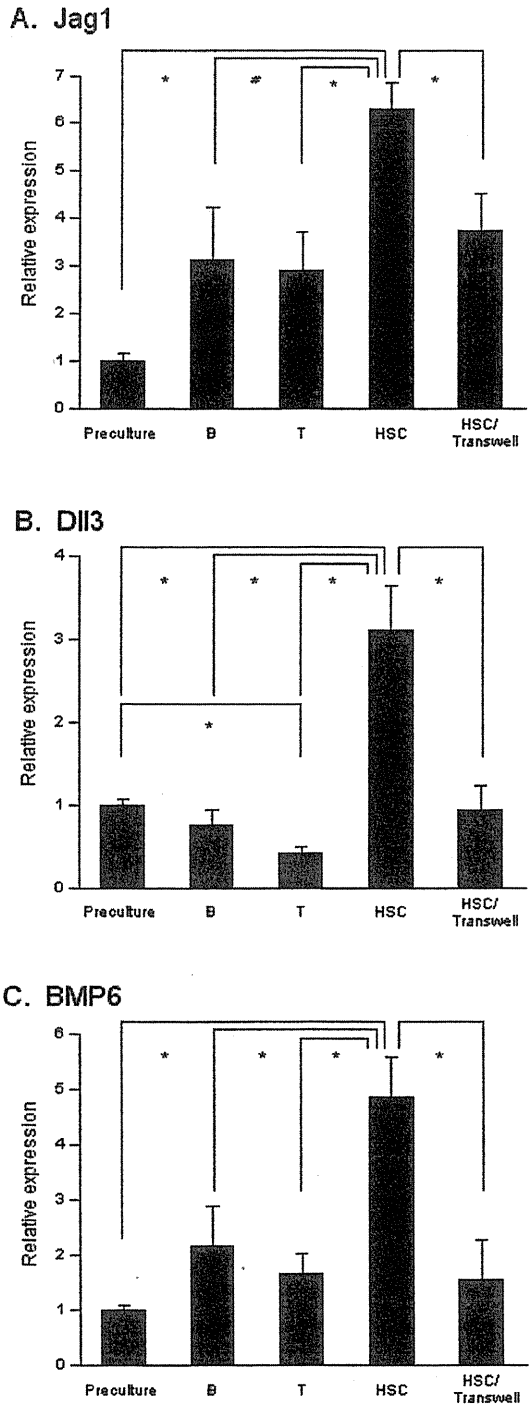

Figure 2. Elevated levels of Jag1, Dll3 and BMP6 in A54 cells cocultured with HSCs. Total RNA was isolated from 2 x 10^4 A54 cells prior to coculture (Preculture) and after 5-day-coculture with 1 x 10^4 B-lymphocytes (B), 1 x 10^4 T-lymphocytes (T) or 1 x 10^4 bone marrow Lin^-Sca1^+ cells (HSC). Expression of Jag1 (A), Dll3 (B) and BMP6 (C) was measured by quantitative RT-PCR with the primers listed in Table 1. HSC/Transwell: A54 cells were coincubated with HSCs but separated by Cell Culture Insert. *: $P < 0.01$ ($n = 3$).

Dll3 expression in A54 was decreased after coculture with T-cells, while it was not significantly changed after coculture with B-cells (Figure 2B). BMP6 expression was mildly upregulated in A54 cells cocultured with mature lymphocytes, but the difference was not statistically significant (Figure 2C). These results suggested that the upregulation of Jag1, Dll3 and BMP6 was induced by interaction with immature hematopoietic cells. Furthermore, such elevation was cancelled out when A54 cells were separated from HSCs with a microporous membrane (Figure 2). Immunostaining with an anti-Jag1 antibody confirmed that hematopoietic progenitors stimulated Jag1 expression in the neighboring A54 preadipocytes. Jag1 signal was apparently greater in A54 cells in cobblestoned areas than those in the surrounding regions (Figure 3). Taken together, mesenchymal stromal cell-derived preadipocytes received signals from HSCs through cell contact, resulting in multiple events including upregulation of Jag1, Dll3 and BMP6.

Activation of Notch signaling in HSCs

The coculture experiment showed that the expression of multiple Notch ligands (Jag1 and Dll3) was upregulated in A54 preadipocytes during their interaction with HSCs. We next addressed whether the expression of Notch receptors and downstream factors was altered in the HSCs.

Figure 3

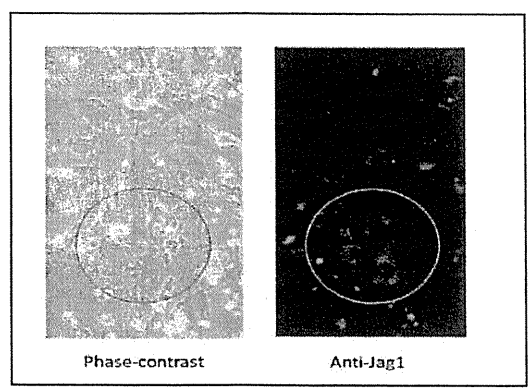

Figure 3. Jag1 expression in a cobblestone area. 1 x 10^4 murine bone marrow HSCs were incubated on 2 x 10^4 A54 cells for 5 days. Cells were immunostained with a rabbit anti-mouse Jag1 antibody and Alexa Fluor 488-conjugated goat anti-rabbit IgG. In the left panel (phase-contrast bright field, magnification × 400), a cobblestone area with small, rounded hematopoietic cells is indicated with a circle. In the right panel (immunofluorescent view, magnification × 400) showing the same location, several large, stretched stromal cells are positively immunostained (green), wheras stromal cells outside the cobblestone area are negative or weakly positive.

Table 2. Hematopoiesis-related genes upregulated or downregulated in cocultured A54 cells.

Upregulated or downregulated molecule	Before [a]	After [b]	Ratio [c]
Upregulated			
Mcl1 (Myeloid cell leukemia sequence 1)	116	514	4.42
Stom (Stomatin)	126	481	3.83
Foxk1 (Forkhead box K1)	129	464	3.58
Foxf2 (Forkhead box F2)	133	455	3.43
Bmp6 (Bone morphogenetic protein-6)	133	451	3.38
Itgbl1 (Integrin , beta-like 1)	135	447	3.30
Dll3 (Delta-like 3)	136	446	3.29
Arts1 (Adipocyte-derived leucine aminopeptidase)	136	446	3.28
Sox13 (SRY-box containing gene 13)	136	444	3.27
Cdc40 (Cell division cycle 40 homolog)	136	443	3.26
Jag1 (Jagged 1)	137	443	3.24
Shh (Sonic hedgehog)	137	440	3.20
Cdc16 (Cell division cycle 16 homolog)	143	423	2.95
Sox17 (SRY-box containing gene 17)	146	416	2.85
Cdc2l6 (Cell division cycle 2-like 6)	144	408	2.83
Col15a1 (procollagen , type XV)	147	408	2.77
Rras (Ras-related protein)	149	405	2.72
Pik3cb (phosphatidylinositol3-kinase, catalytic, b polypeptide)	147	401	2.72
Hoxa3 (Homeobox A3)	149	378	2.54
Adfp (Adipophilin, Adipose differentiation-related protein)	150	361	2.41
Cdc91l1 (cell division cycle 91-like 1)	146	324	2.22
Downregulated			
Nudt2 (nucleoside diphosphate linked moiety X - type motif 2)	3155	1337	0.42
Lrp2 (LDL receptor-related protein 2)	2210	963	0.44
TPO (thrombopoietin)	866	419	0.48
Taar1 (trace amine-associated receptor 1)	892	432	0.48
Centg3 (centaurin , gamma 3)	1932	942	0.49
Ccdc66	777	382	0.49
Olig1 (oligodendrocyte transcription factor 1)	1293	639	0.49
AA474455	1809	897	0.49

[a] Before: Expression (net intensity) in A54 cells before coculture.
[b] After: Expression in A54 cells after 3 days of coculture with HSCs.
[c] Ratio = After/Before.

A quantitative RT-PCR analysis revealed that the message level of Notch1 was elevated in HSCs cocultured with A54 cells by 3.6-fold (Figure 4A). Simultaneously, the expression of Hairy enhancer of split-1 (Hes1), a target of Notch1, was upregulated by 27-fold, indicating that the authentic signaling pathway was actually viable (Figure 4B). The results clearly showed that Notch ligands and receptors were upregulated in the stromal cells and HSCs in a reciprocal fashion through cell contact.

Discussion

In the present study, we investigated the molecular events in hematopoiesis supported by mesenchymal stromal cell-derived preadipocytes. We and other investigators reported that several preadipocyte-like stromal cells were capable of supporting hematopoiesis [13–16]. While osteoblasts enhance HSC self-renewal in the hematopoietic niche [2,3], preadipocytes may have additional or different function, such as promoting the asymmetric division of HSCs and proliferation of early progenitors. Our finding that A54 preadipocytes promoted the formation of cobblestone areas and colonies supports this idea, but such function may not be completely cell-autonomous. Assuming that some instructive signals from HSCs, we investigated the gene expression profile of A54 cells in a coculture with HSCs. Among the molecules upregulated or downregulated by more than twofold in a microarray screening, an increase of Notch ligands (Jag1 and Dll3) and BMP6 was confirmed in A54 cells. This finding is intriguing, because signals from Notch and BMP receptors are integrated in osteoblasts and other cell types [17-20]. Notch is a single-pass transmembrane receptor interacting with cell-bound ligands. So far, four Notch receptors (Notch1-4) and five ligands (Jag1-2 and Dll1, 3 and 4) have been identified in mammals. As in many cell systems, Notch signaling is essential for regulating HSCs and blood cell differentiation [21,22].

Previous studies showed that Jag1 in marrow stromal cells and osteoblasts promotes HSC proliferation [3,23], Dll1 produces cobblestone areas [24]. In the present study, we demonstrated that coculturing resulted in concomitant increases in Notch ligands (Jag1 and Dll3) in A54 preadipocytes and Notch signaling in HSCs. Notably, in accordance with an elevation in levels of the Notch1 receptor, expression of the transcription factor Hes1 was also upregulated. Hes1, one of the targets of Notch signaling, regulates specific groups of genes to maintain HSCs and early progenitors [25,26]. Thus, upregulation of the Notch1-Hes1 axis in HSCs strongly suggests that this signaling pathway is actually viable with the increase in Notch ligands in neighboring preadipocytes. Since Notch activation plus cytokine receptor signaling has a combined effect on hematopoietic cells [27], production of Notch ligands and cytokines (SCF, SDF1 and Ang1) by A54 cells is likely to represent a physiological role of marrow niche cells.

Figure 4

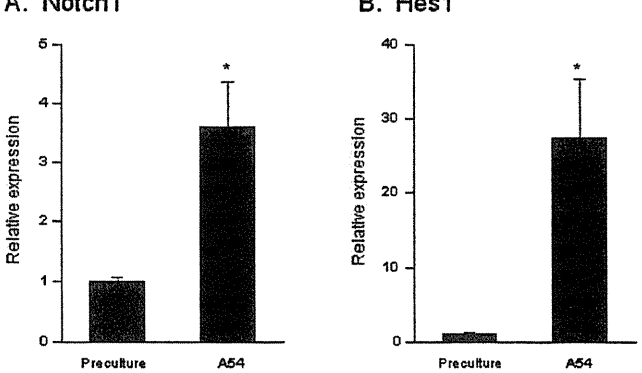

Figure 4. Expression of Notch1 and Hes1 in HSCs. Total RNA was isolated from 1 x 10^4 bone marrow Lin^-Sca1^+ cells prior to coculture and after 5-day-coculture with 2 x 10^4 A54 cells. Notch1 and Hes1 message levels were estimated by quantitative RT-PCR before (Preculture) and after coculture with A54 preadipocyres (A54). The primers for PCR are listed in Table 1. Both Notch1 (A) and Hes1 (B) were significantly upregulated in HSCs after coculture with A54 cells. * : $P < 0.01$ ($n = 4$).

Figure 5

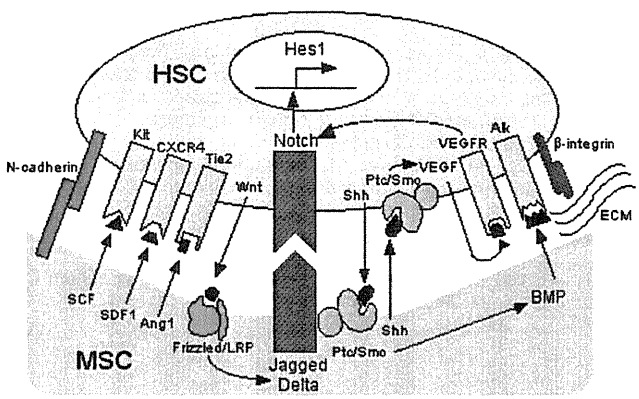

Figure 5. Interaction of MSCs and HSCs. Various factors are involved in the cell-to-cell interaction between MSCs and HSCs with spatial and temporal complexity. HSCs attach to MSCs via adhesion molecules such as N-cadherin and b-integrins (ECM: extracellular matrix secreted from MSC-derived cells). Soluble cytokines from MSCs such as SCF, SDF1 and Ang1 support the growth and differentiation of HSCs through cognate receptors (Kit, CXCR4 and Tie2). When HSCs and MSCs are in close proximity, expression of Notch ligands (Jagged and Delta-like) is upregulated in MSCs by Wnt from HSCs, while that of Notch receptors is upregulated in HSCs by Sonic hedgehog (Shh) from MSCs and HSCs. Vascular endothelial growth factor (VEGF) can further upregulate Notch receptor expression in an autocrine or paracrine fashion. The upregulated Notch signaling pathway induces the expression of downstream targets such as Hes1. The expression of bone morphogenic protein (BMP) is upregulated in MSCs by Shh signaling. Frizzled, Ptc/Smo, VEGFR, Alk: receptors for Wnt, Shh, VEGF and BMP, respectively.

Bone morphogenetic proteins (BMPs) belong to the transforming growth factor-b superfamily and have pleiotropic effects on tissue development. They have been implicated as key regulators in hematopoiesis: for example, BMP4 promotes the self-renewal of HSCs [28] and BMP6 enhances the formation of colonies [17]. Because of the redundancy of ligands/receptors and the dependence on the context and stage of differentiation of target cells, a detailed understanding of BMP signaling awaits further investigation.

The mechanisms responsible for the reciprocal upregulation of the expression of Notch ligands and receptors have yet to be clarified. We found that mature lymphocytes poorly induced Jag1, Dll3 and BMP6 expression in A54 cells, thus the stromal cells appear to receive the induction signal mainly from immature cells such as HSCs. Direct cell-to-cell contact with, or close proximity to HSCs was required for the upregulation of Jag1, Dll3 and BMP6 expression in A54 cells. Thus far several classes of molecules have been implicated to act upstream of Notch signaling. For example, the Wnt canonical pathway regulates the expression of Notch ligands in various cell types [29-31]. Sonic hedgehog (Shh) and receptors for Shh (Ptc/Smo) are expressed on primitive hematopoietic cells and marrow stromal cells and induce BMP expression [32,33]. In addition, Shh can increase levels of Notch receptors via vascular endothelial growth factor (VEGF) [34]. Of note, Wnt and Shh are lipid-modified proteins, and therefore appropriate for exerting effects on short-ranged target cells in a paracrine and/or autocrine fashion [35,36]. In the hematopoietic niche, these signaling networks must be precisely orchestrated to regulate HSC behavior, presumably through cross-talk with signals from adhesion molecules such as integrins (Figure 5). Further investigation of such communicative events will identify target molecules to improve engraftment in transplantation therapy.

References

1. Schofield R. The relationship between the spleen colony-forming cell and the haemopoietic stem cell. Blood Cells 1978; 4: 7-25.
2. Zhang J, Niu C, Ye L, Huang H, He X, Tong W-G, Ross J, Haug J, Johnson T, Feng JQ, Harris S, Wiedemann LM, Mishina Y, Li L. Identification of the haematopoietic stem cell niche and control of the niche size. Nature 2003; 425: 836-841.
3. Calvi LM, Adams GB, Weibrecht KW, Weber JM, Olson DP, Knight MC, Martin RP, Schipani E, Divieti P, Bringhurst FR, Milner LA, Kronenberg HM, Scadden DT. Osteoblastic cells regulate the haematopoietic stem cell niche. Nature 2003; 425: 841-846.
4. Kiel MJ, Yilmaz ÖH, Iwashita T, Yilmaz OH, Terhorst C, Morrison SJ. SLAM family receptors distinguish hematopoietic stem and progenitor cells and reveal endothelial niches for stem cells. Cell 2005; 121: 1109-1121.
5. Heissig B, Hattori K, Dias S, Friedrich M, Ferris B, Hackett NR, Crystal RG, Besmer P, Lyden D, Moore MAS, Werb Z, Rafii S. Recruitment of stem and progenitor cells from the bone marrow niche requires MMP-9 mediated release of Kit-ligand. Cell 2002; 109: 625-637.
6. Ara T, Tokoyoda K, Sugiyama T, Egawa T, Kawabata K, Nagasawa T. Long-term hematopoietic stem cells require stromal cell-derived factor-1 for colonizing bone marrow during ontogeny. Immunity 2003; 19: 257-267.
7. Hattori K, Heissig B, Tashiro K, Honjo T, Tateno M, Shieh J-H, Hackett NR, Quitoriano MS, Crystal RG, Rafii S, Moore MAS. Plasma elevation of stromal cell-derived factor-1 induces mobilization of mature and immature hematopoietic progenitor and stem cells. Blood 2001; 97: 3354-3360.
8. Arai F, Hirao A, Ohmura M, Sato H, Matsuoka S, Takubo K, Ito K, Koh GY, Suda T. Tie2/Angiopoietin-1 signaling regulates hematopoietic stem cell quiescence in the bone marrow niche. Cell 2004; 118: 149-161.
9. Stier S, Ko Y, Forkert R, Lutz C, Neuhaus T, Grünwald E, Chen T, Dombkowski D, Calvi LM, Rittling SR, Scadden DT. Osteopontin is a hematopoietic stem cell niche component that negatively regulates stem cell pool size. J Exp Med 2005; 201: 1781-1791.
10. Wagner W, Saffrich R, Wirkner U, Eckstein V, Blake J, Ansorge A, Schwager C, Wein F, Milesala K, Ansorge W, Ho AD. Hematopoietic progenitor cells and cellular microenvironment: behavioral and molecular changes upon interaction. Stem Cells 2005; 37: 1180-1191.
11. Pittenger MF, Mackay AM, Beck SC, Jaiswal RK, Douglas R, Mosca JD, Moorman MA, Simonetti DW, Craig S, Marshak. Multilineage potential of adult human mesenchymal stem cells. Science 1999; 284: 143-147.
12. Wagner W, Wein F, Roderburg C, Saffrich R, Faber A, Krause U, Schubert M, Benes V, Eckstein V, Maul H, Ho AD. Adhesion of hematopoietic progenitor cells to human mesenchymal stem cells as a model for cell-cell interaction. Exp Hematol 2007; 35: 314-325.
13. Nishikawa M, Ozawa K, Tojo A, Yoshikubo T, Okano A, Tani K, Ikebuchi k, Nakauchi H, Asano S. Changes in hematopoiesis-supporting ability of C3H10TI/2 mouse embryo fibroblasts during differentiation. Blood 1993; 81: 1184-1192.
14. Oh I, Ozaki K, Miyazato A, Sato K, Meguro A, Muroi K, Nagai T, Mano H, Ozawa K. Screening of genes responsible for differentiation of mouse mesenchymal stromal cells by DNA micro-array analysis of C3H10T1/2 and C3H10T1/2-derived cell lines. Cytotherapy 2007; 9: 80-90.
15. Yoshikubo T, Ozawa K, Takahashi K, Nishikawa M, Horiuchi N, Tojo A, Tani K, Kodama H, Asano S. Adhesion of NFS-60 myeloid leukemia cells to MC3T3-G2/PA6 stromal cells induces granulocyte colony-stimulating factor production. Blood 1994; 84: 415-420.
16. Nakamura M, Harigaya K, Watanabe Y. Correlation between production of colony-stimulating activity (CSA) and adipose conversion in a murine marrow-derived preadipocyte line (H-1/A). Proc Soc Exp Biol Med 1985; 179: 283-287.
17. Detmer K, Walker AN. Bone morphogenetic proteins act synergistically with haematopoietic cytokines in the differentiation of haematopoietic progenitors. Cytokine 2002; 17: 36-42.
18. Nobta M, Tsukazaki T, Shibata T, Xin C, Moriishi T, Sakano S, Shindo H, Yamaguchi A. Critical regulation of bone morphogenic protein-induced osteoblastic differentiation by Delta1/Jagged1-activated Notch1 signaling. J Biol Chem 2005; 280: 15842-15848.
19. Katoh M, Katoh M. Transcriptional regulation of WNT2B based on the balance of Hedgehog, Notch, BMP and WNT signals. Int Natl J Oncol 2009; 34: 1411-1415.
20. Blank U, Karlsson S. Signaling pathways governing cell fate. Blood 2009; 111: 492-503.
21. Chiba S. Notch signaling in stem cell systems. Stem Cells 2006; 24: 2437-2447.

22. Weber JM, Calvi LM. Notch signaling and the bone marrow hematopoietic stem cell niche. Bone 2010; 46: 281-285.
23. Duncan AW, Rattis FM, DiMascio LN, Congdon KL, Pazianos G, Zhao C, YoonK, Cook JM, Willert K, Gaiano N, Reya T. Integration of Notch and Wnt signaling in hematopoietic stem cell maintenance. Nature Immunol 2005; 6: 314-322.
24. Moore KA, Pytowski B, Witte L, Hicklin D, Lemischka I. Hematopoietic activity of a stromal cell transmembrane protein containing epidermal growth factor-like repeat motifs. Proc Natl Acad Sci USA 1997; 94: 4011-4016.
25. Kunisato A, Chiba S, Nakagami-Yamaguchi E, Kumano K, Saito T, Masuda S, Yamaguchi T, Osawa M, Kageyama R, Nakauchi H, Nishikawa M, Hirai H. HES-1 preserves purified hematopoietic stem cell ex vivo and accumulates side population cells in vivo. Blood 2003; 101: 1777-1783.
26. Yu X, Alder JK, Chun JH, Friedman AD, Heimfeld S, Cheng L, Civin CI. HES1 inhibits cycling of hematopoietic progenitor cells via DNA binding. Stem Cells 2006; 24: 876-888.
27. Varnum-Finney B, Xu L, Brashem-Stein C, Nourrigat C, Flowers D, Bakkour S, Pear WS, Bernstein ID. Pluripotent, cytokine-dependent, hematopoietic stem cells are immortalized by constitutive Notch1 signaling. Nat Med 2000; 6: 1278-1281.
28. Bhatia M, Bonnet D, Wu D, Murdoch B, Wrana J, Gallacher L, Dick JE. Bone morphogenetic proteins regulate the developmental program of human hematopoietic stem cells. J Exp Med 1999; 189: 1139-1148.
29. Murdoch B, Chadwick K, Martin M, Shojaei F, Shah KV, Gallacher L, Moon RT, Bhatia M. Wnt-5A augments repopulating capacity and primitive hematopoietic development of human blood stem cells in vivo. Proc Natl Acad Sci USA 2003; 100: 3422-3427.
30. Katoh M, Katoh H. Notch ligand, JAG1, is evolutionarily conserved target of canonical WNT signaling pathway in progenitor cells. Int J Mol Med 2006; 17: 681-685.
31. Estrach S, Ambler CA, Lo Celso C, Hozumi K, Watt FM. Jagged 1 is a b-catenin target gene required for ectopic hair follicle formation in adult epidermis. Development 2006; 133: 4427-4438.
32. Bhardwaj G, Murdoch B, Wu D, Baker DP, Williams KP, Chadwick K, Ling LE, Karanu FN, Bhatia M. Sonic hedgehog induces the proliferation of primitive hematopoietic cells via BMP regulation. Nat Immunol 2001; 2: 172-180.
33. Katoh Y, Katoh M. Hedgehog signaling pathway and gastrointestinal stem cell signaling network (review). Int J Mol Med 2006; 18: 1019-1023.
34. Lawson ND, Vogel AM, Weinstein BM. Sonic hedgehog and vascular endothelial growth factor act upstream of the notch pathway during arterial endothelial differentiation. Dev Cell 2002; 3: 127-136.
35. Willert K, Brown JD, Danenberg E, Duncan AW, Weissman IL, Reya T, Yates JR III, Nusse R. Wnt proteins are lipid-modified and can act as stem cell growth factors. Nature 2003; 423: 448-452.
36. Porter JA, Young KE, Beachy PA. Cholesterol modification of Hedgehog signaling proteins in animal development. Nature 1996; 274: 255-259.

Grants

This work was supported in part by grants-in-aid for scientific research from the Ministry of Health, Labour and Welfare, and the Ministry of Education, Culture, Sports, Science and Technology of Japan.

Correspondence to be addressed to:

* Akihiro Kume, M.D., Ph.D., Division of Genetic Therapeutics, Center for Molecular Medicine, Jichi Medical University. 3311-1 Yakushiji, Shimotsuke, Tochigi 329-0498, Japan. Tel: +81-285-58-7402; Fax: +81-285-44-8675; Email: kume@jichi.ac.jp, eternalricenikko98@gmail.com

A putative inhibitory mechanism in the tenase complex responsible for loss of coagulation function in acquired haemophilia A patients with anti-C2 autoantibodies

Tomoko Matsumoto; Keiji Nogami; Kenichi Ogiwara; Midori Shima
Department of Pediatrics, Nara Medical University, Kashihara, Japan

Summary

Acquired haemophilia A (AHA) is caused by the development of factor (F)VIII autoantibodies, demonstrating type 1 or type 2 inhibitory behaviour, and results in more serious haemorrhagic symptoms than in congenital severe HA. The reason(s) for this remains unknown, however. The global coagulation assays, thrombin generation tests and clot waveform analysis, demonstrated that coagulation parameters in patients with AHA-type 2 inhibitor were more significantly depressed than those in patients with moderate HA with similar FVIII activities. Thrombin and intrinsic FXa generation tests were significantly depressed in AHA-type 1 and AHA-type 2 compared to severe HA, and more defective in AHA-type 1 than in AHA-type 2. To investigate these inhibitory mechanism(s), anti-FVIII autoantibodies were purified from AHA plasmas. AHA-type 1 autoantibodies, containing an anti-C2 ESH4-epitope, blocked FVIII(a)-phospholipid binding, whilst AHA-type 2, containing an anti-C2 ESH8-epitope, inhibited thrombin-catalysed FVIII activation. The coagulation function in a reconstituted AHA-model containing exogenous ESH4 or ESH8 was more abnormal than in severe HA. The addition of anti-FIX antibody to FVIII-deficient plasma resulted in lower coagulation function than its absence. These results support the concept that global coagulation might be more suppressed in AHA than in severe HA due to the inhibition of FIXa-dependent FX activation by steric hindrance in the presence of FVIII-anti-C2 autoantibodies. Additionally, AHA-type 1 inhibitors prevented FVIIIa-phospholipid binding, essential for the tenase complex, whilst AHA-type 2 antibodies decreased FXa generation by inhibiting thrombin-catalysed FVIII activation. These two distinct mechanisms might, in part, contribute to and exacerbate the serious haemorrhagic symptoms in AHA.

Keywords

Acquired haemophilia A, anti-C2 autoantibody, thrombin generation, tenase complex, FXa generation

Correspondence to:
Keiji Nogami, MD, PhD
Department of Pediatrics, Nara Medical University
840 Shijo-cho, Kashihara, Nara 634–8522, Japan
Tel.: +81 744 29 8881, Fax: +81 744 24 9222
E-mail: roc-noga@naramed-u.ac.jp

Presented in abstract form at the 52nd annual meeting of the American Society of Hematology, Orlando, Florida, USA, December 6, 2010.

Financial support:
This work was partly supported by the grants for Bayer Hemophilia Award, 2009 and MEXT KAKENHI 21591370, 2009.

Received: May 16, 2011
Accepted after major revision: November 20, 2011
Prepublished online: January 11, 2012
doi:10.1160/TH11-05-0331
Thromb Haemost 2012; 107: ■■■

Introduction

Factor (F)VIII, a protein deficient or defective in individuals with severe congenital bleeding disorder, haemophilia A (HA), functions as a cofactor in the tenase complex, responsible for phospholipid (PL)-dependent conversion of FX to FXa by FIXa (1). FVIII circulates as a complex with von Willebrand factor (VWF) that protects and stabilises the cofactor (2). FVIII is synthesised as a single chain molecule consisting of 2,332 amino acid residues, and is arranged into three domains, A1-A2-B-A3-C1-C2. FVIII is processed into a series of metal ion-dependent heterodimers, generating a heavy chain (HCh) consisting of A1 and A2 domains together with heterogenous fragments of partially proteolysed B domain linked to a light chain (LCh) consisting of A3, C1, and C2 domains (3). The catalytic efficiency of FVIII in the tenase complex is markedly enhanced by conversion into FVIIIa, by limited proteolysis by thrombin (and FXa) (4). Both enzymes proteolyse the HCh at Arg^{372} and Arg^{740}, and produce 50-kDa A1 and 40-kDa A2 subunits. The 80-kDa LCh is cleaved at Arg^{1689} generating a 70-kDa subunit. Proteolysis at Arg^{372} and Arg^{1689} is essential for generating FVIIIa cofactor activity (5). FVIIIa activity is down-regulated by serine proteases including activated protein C, following cleavage at Arg^{336} (4, 6).

FVIII inhibitors develop as alloantibodies (alloAbs) in severe HA patients multi-treated with FVIII concentrates, and also as autoantibodies (autoAbs) in previously normal individuals, particularly in elderly people, patients with autoimmune diseases, pregnant women, and women in the postpartum period. The appearance of autoAbs usually results in severe haemorrhagic symptoms in what is described as acquired HA (AHA). Antibodies of this nature inhibit FVIII activity (FVIII:C) either completely or incompletely at saturating concentrations, corresponding to type 1

or type 2 inhibitors, respectively (7). Epitopes of autoAbs and haemophilic alloAbs have been found commonly in the A2, C2, or both domains of the FVIII molecule (8). Most autoAbs appear to be directed against a single domain rather than both domains, with anti-C2 antibodies being more common than anti-A2 antibodies (8). In contrast, most haemophilic alloAbs appear to recognise both domains. Anti-C2 type 1 antibodies inhibit FVIIIa binding to PL membranes (9, 10). The FVIII binding to PL and VWF is mutually exclusive (11), and antibodies have been shown to block binding to both PL and/or VWF (12, 13). Furthermore, anti-C2 type 2 antibodies interfere with FVIII activation mediated by thrombin and/or FXa (9, 10, 14).

Accurate measurements of blood coagulation *in vitro* are essential for the complete clinical assessment of clotting function. Conventional one-stage clotting tests (prothrombin time and activated partial thromboplastin time; APTT) are useful for routine laboratory examination, but they only partially reflect coagulation in a non-physiological environment and are based on the classical concepts of intrinsic and extrinsic cascade mechanisms. Discrepancies between coagulant activity and clinical phenotype in patients are often apparent, therefore. Recently, interest has focused on global coagulation assays, developed from a better understanding of the coagulation reaction involving tissue factor (TF)-triggered, cell-based mechanisms generating thrombin on activated platelets (15). Global tests of this nature such as the thrombin generation test (TGT) and clot waveform analysis have been established (16–18). We have further reported that our optimisation of these techniques provided a quantitative evaluation of clotting function in patients with very low levels of FVIII:C, and that various parameters closely correlated with clinical phenotype (18–20).

According to a retrospective survey, the severity of AHA is not directly associated with FVIII:C level (21), and AHA patients frequently present with life- or limb-threatening bleeding episodes that appear to be more pronounced than in congenital HA, although FVIII:C levels are similar in both. Hence, the clinical phenotype is often severe in AHA patients with moderate or even mildly deficient levels of FVIII:C. The reason(s) for this discrepancy in AHA remains to be clarified, however.

In the present study, patients with moderate-type HA (M-group), severe-type HA (S-group), AHA with type 1 (type 1) and with type 2 inhibitors (type 2) were investigated. We have demonstrated for the first time that coagulation function, assessed using global coagulation assays, was significantly more depressed in AHA with anti-C2 autoAbs compared to congenital HA, particularly in the S-group. We propose that one possibility for this difference is that the complex of FVIII and anti-C2 autoAbs indirectly interferes with FIXa-dependent FX activation due to steric hindrance. In addition, type 1 anti-C2 autoAbs prevented FVIII(a)-PL binding mechanisms, essential for the tenase complex, and type 2 anti-C2 autoAbs decreased FXa generation by inhibiting FVIII activation mediated by thrombin (and/or FXa). These distinct mechanisms might be associated with the exacerbated haemorrhagic symptoms in AHA.

Materials and methods

Reagents

An anti-FVIII A2 mAbJR8 was obtained from JR Scientific Inc. (Woodland, CA, USA). Anti-FVIII C2 mAbs, ESH4 and ESH8, recognising residues 2303–2332 and residues 2248–2285, respectively (12, 22), were purchased from American Diagnostica Inc. (Stamford, CT, USA). An anti-C2 alloAb was purified from plasma obtained in a severe HA patient with inhibitor. An anti-FIX mAb3A6 was prepared as previously reported (23). The biotinylation of mAb was prepared using *N*-hydroxysuccinimido-biotin (Pierce, Rockford, IL, USA). Recombinant lipidated TF (Innovin®; Dade Behring, Marburg, Germany), ellagic acid (Sysmex, Kobe, Japan), thrombin-specific fluorogenic substrate (Bachem, Bubendorf, Switzerland), and thrombin calibrator (Thrombinoscope, Maastricht, Netherlands) were obtained from the indicated vendors. Human thrombin, FV, FIXa, FX, FXa (Hematologic Technologies, Inc. Essex, VT, USA), recombinant hirudin (Calbiochem, San Diego, CA, USA), FXa substrate S-2222 and thrombin substrate S-2238 (Chromogenix, Milano, Italy), and plasma-derived FVIII-deficient plasma (George King Biomedical. Overland Park, KS, USA) were commercially purchased. PL vesicles containing 10% phosphatidylserine, 60% phosphatidylcholine, 30% phosphatidylethanolamine (Sigma) were prepared as previously described (24).

Proteins

Purified recombinant (r)FVIII preparations (Kogenate FS®) were a generous gift from Bayer Corp. Japan (Osaka, Japan). The A1, A2, HCh, LCh, and thrombin-cleaved LCh fragments were isolated from recombinant FVIII (25). The rA3 and rC2 proteins were purified as previously reported (26, 27). VWF was purified from FVIII/VWF concentrates (28). SDS-PAGE of the isolated subunits followed by staining with GelCode Blue Stain Reagent (Pierce) showed >95% purity (data not shown). Protein concentrations were measured using the Bradford method (29).

Patients' plasmas

Whole blood was obtained by venipuncture into tubes containing 1:9 volume of 3.8% (w/v) trisodium citrate. After centrifugation for 15 minutes (min) at 1,500 g, the plasmas were stored at –80°C, and thawed at 37°C immediately prior to the assays. Inhibitor titres were determined using the Bethesda assay (30). The kinetic pattern (type 1 or type 2 behaviour) of FVIII inactivation by anti-FVIII autoAbs was determined using one-stage clotting assays (7). Patients' plasmas were obtained from moderate-type HA (M-group, n=10, FVIII:C: 2.1 ± 0.9 IU/dl), severe-type HA (S-group, n=15, FVIII:C: <0.2 IU/dl), type 1 AHA (type 1, n=9, FVIII:C: <0.2 IU/

dl, 167 ± 175 BU/ml) and type 2 AHA (type 2, n=8, FVIII:C: 2.0 ± 1.9 IU/dl, 202 ± 120 BU/ml). The present studies were performed using blood samples obtained from patients diagnosed by our research group (Table 1) and enrolled in the Nara Medical University Hemophilia Program. All samples were obtained after informed consent following local ethical guidelines.

Anti-FVIII autoAbs

Anti-FVIII autoAb IgGs were purified from AHA plasma. IgG preparations were fractionated by affinity chromatography on protein G-Sepharose. $F(ab')_2$ fragments were prepared using immobilised pepsin-Sepharose (Pierce) (31). The FVIII domain(s) recognised by these antibodies were determined by SDS-PAGE and Western blotting using isolated FVIII fragments. The binding of anti-FVIII antibodies to FVIII fragments was detected using anti-human peroxidase-linked secondary antibody (Dako Japan, Tokyo, Japan). All autoAbs reacted predominantly or exclusively with the C2 domain in these immunoblot analyses using isolated FVIII fragments. Little reaction was evident with coagulant proteins other than FVIII (data not shown). All of these autoAbs, therefore, were regarded as anti-C2 autoAbs.

Clot waveform analysis

FVIII(a) activity was measured in one-stage clotting assay using FVIII-deficient plasma. APTT measurements were also performed using the MDA-II™ Hemostasis System (Trinity Biotech, Dublin, Ireland) with commercially available APTT reagent. The clot waveforms obtained were computer-processed using the commercial kinetic algorithm (18). The minimum value of the first derivative (min1), defining the maximum velocity of change in light transmission, was calculated as an indicator of the maximum velocity of coagulation achieved. The second derivative of the transmittance data (d^2T/dt^2) reflects the acceleration of the reaction at any given time point. The minimum value of the second derivative (min2) was also calculated as an index of the maximum acceleration of the reaction achieved. Since the minimum of min1 and min2 are derived from negative changes, we expressed the data as |min1| and |min2|, respectively. The clot time was defined as the time until the start of coagulation.

Thrombin generation test (TGT)

The calibrated automated TGT (Thrombinoscope) was performed as previously described (16, 20). Sample plasma (80 µl) was pre-incubated for 10 min with 20 µl of trigger reagent containing TF, PL, and ellagic acid (final concentration (f.c.) 0.5 pM, 4 µM, and 0.3 µM, respectively). Measurements were then commenced after the addition of 20 µl reagent containing $CaCl_2$ and fluorogenic substrate (f.c. 16.7 mM and 2.5 mM, respectively). The development of fluorescent signals was monitored using a Fluoroskan Ascent microplate reader (Thermo Fisher Scientific, Boston, MA, USA). Data analyses were performed using the manufacture's software, and the standard parameters; peak thrombin, time to peak, and endogenous thrombin potential (ETP), were derived.

Table 1: Properties of plasma samples and anti-C2 autoAbs obtained from AHA patients.

Case	FVIII:C (IU/dl)	FVIII:Ag (IU/dl)	Inhibitor (BU/ml)	Kinetic pattern	Recognition	
					Coagulant factor	Epitope*
1	<0.2	1.0	30.7	type 1	FVIII	C2
2	<0.2	<1.0	1,100	type 1	FVIII	C2
3	<0.2	<1.0	48.8	type 1	FVIII	C2,(A2)
4	<0.2	<1.0	110	type 1	FVIII	C2
5	<0.2	11.1	32.7	type 1	FVIII	C2,(A2)
6	<0.2	<1.0	135	type 1	FVIII	C2
7	<0.2	6.5	33.1	type 1	FVIII	C2
8	<0.2	<1.0	65.3	type 1	FVIII	C2
9	<0.2	11.2	36.8	type 1	FVIII	C2
10	1.1	1.0	8.2	type 2	FVIII	C2
11	1.2	1.0	33.0	type 2	FVIII	C2
12	1.2	29.0	7.9	type 2	FVIII	C2
13	1.4	1.0	860	type 2	FVIII	C2,(A2)
14	1.5	2.8	300	type 2	FVIII	C2
15	6.4	14.1	1.2	type 2	FVIII	C2
16	1.0	10.0	31.7	type 2	FVIII	C2
17	3.2	2.4	10.6	type 2	FVIII	C2

Type 1 or Type 2 antibodies inhibit FVIII:C either completely or incompletely at saturating concentrations. *: Cases 3, 5, and 13 reacted very faintly with the A2 domain.

FXa generation assay

FXa generation was performed at 37°C in 20 mM HEPES, pH 7.2, 150 mM NaCl, 5 mM $CaCl_2$, and 0.01% Tween 20 (HBS) containing 0.1% bovine serum albumin (BSA).

Purified reagent-based assays

(i) FVIIIa/FIXa-dependent FXa generation (32) – FVIII (0.05 nM) was activated by thrombin (1 nM), and this reaction was terminated after 1 min by the addition of hirudin (0.5 unit/ml). After dilution, FXa generation was initiated by the addition of FIXa (1 nM), FX (150 nM), and PL (20 µM).

(ii) FVIII/FIXa-dependent FXa generation – FXa generation was initiated by the addition of FIXa (1 nM), FX (150 nM), PL (20 μM), and hirudin (0.5 unit/ml) to FVIII (0.05 nM) and continued for 30 min. In both assays, aliquots were removed at the indicated times to assess initial rates of product formation, and added to tubes containing EDTA. Initial rates of FXa generation were determined at 405 nm after the addition of S-2222.

Plasma-based assays

A commercial COATEST®SP FVIII kit (Chromogenix) was used according to the manufacture's instructions. Plasma samples were diluted five fold in HBS containing 0.1% BSA and were mixed with FIXa/FX/PL. FXa generation was initiated by the addition of $CaCl_2$, and the initial rates were determined at 405 nm after the addition of S-2765. Hirudin (1 unit/ml) was added to the samples to stop positive-feedback activation mediated by the generated thrombin.

FVIII competitive binding assay

FVIII (25 nM) in 10 mM Tris and 150 mM NaCl, pH7.4, was immobilised onto microtiter wells at 4°C overnight. After blocking with 5% BSA at 37°C for 2 hours (h), serial dilutions of anti-C2 autoAbs together with constant concentrations (10 μg/ml) of anti-C2 mAbESH4 or mAbESH8 were added to each well, and were further incubated for 2 h. Bound mAbESH4 or mAbESH8 was detected after 2-h incubation with horseradish peroxidase-conjugated anti-mouse IgG and the addition of *o*-phenylenediamine. The amount of nonspecific IgG binding without FVIII was <5% of the total signal. Specific binding was estimated by subtracting the amount of non-specific binding.

ELISA for FVIII binding to immobilised VWF or PL

Binding of FVIII to VWF or PL were examined as previously reported (28). VWF (40 nM) or PL (20 μM) was immobilised onto microtiter wells. After blocking with 5% BSA, FVIII (1 nM) was added onto the immobilised VWF well or PL well. Bound FVIII was detected using biotinylated anti-A2 mAbJR8 and horseradish peroxidase-labeled streptavidin. The amount of non-specific IgG binding without FVIII was <3% of the total signal. Specific binding was estimated by subtracting the amount of non-specific binding.

FVIII cleavage by thrombin or FXa

FVIII (10 nM) was preincubated with the indicated concentrations of anti-C2 autoAbs for 1 h. The mixtures were then incubated at 37°C with thrombin (5 nM) or FXa (0.3 nM) together with PL (20 μM) in HBS-buffer containing 5 mM $CaCl_2$. Aliquots were removed at the indicated times and the reactions were terminated and prepared for SDS-PAGE by adding SDS and boiling for 3 min. SDS-PAGE was performed using 8% gels at 150 V for 1 h, followed by Western blotting. Protein bands were probed using the indicated mAb followed by goat anti-mouse peroxidase-linked secondary mAb. Signals were detected using enhanced chemiluminescence (PerkinElmer Life Science, Boston, MA, USA). Densitometric scans were quantitated using Image J 1.38.

Statistical analysis

The significant of the differences between each of AHA groups, congenital HA groups and samples with anti-C2 mAbs were determined by paired Student's t-test analysis.

Results

Global blood coagulation in moderate HA (M-group) and AHA-type 2

AHA-type 2 patients exhibited more severe haemorrhagic symptoms than the HA M-group, although similar levels of FVIII:C were recorded in one-stage clotting assays. The TGT has been recently developed to evaluate global coagulation function based on the principles of cell-based clotting, and we utilised this technique in this study. Although TF at low concentration is generally used as a trigger in the TGT, sensitive differences in coagulation function at low levels of FVIII:C (<~3 IU/dl) are not seen (20). We have reported, however, that the addition of small amounts of ellagic acid to the mixtures containing the low TF-trigger TGT had little effect on the lag-time (representing activation of the FVIIa/TF-induced extrinsic pathway) but provided higher peak thrombin and ETP measurements (representing the subsequent activation of the intrinsic pathway) (20). The modified TGT, therefore, reflected global coagulation sensitivity in the intrinsic pathway as well as the extrinsic, cell-based pathway, and enabled evaluation of coagulation function at very low levels of FVIII:C (low limit; <0.4 IU/dl).

This TGT was utilised in the present study and plasma samples were mixed with TF (0.5 pM), PL (4 μM), and ellagic acid (0.3 μM), followed by the addition of $CaCl_2$ and fluorogenic substrate (20). Representative thrombograms (*upper panels*) and the derived parameters (*lower panels*) in the M-group and type 2 AHA are illustrated in ▶ Figure 1A. The levels of peak thrombin and ETP obtained in type 2 were significantly decreased relative to those in the M-group, by ~2.6-fold (type 2/M-group: 61 ± 30/159 ± 50 nM, $p<0.01$; *panel* a) and by ~2.2-fold (1,310 ± 810/2,848 ± 620 nM, $p<0.01$; *panel* c), respectively. The time to peak was markedly prolonged by ~1.9-fold (32.2 ± 5.8/17.1 ± 2.0 min, $p<0.01$; *panel* b).

Global coagulations parameters in both groups were further

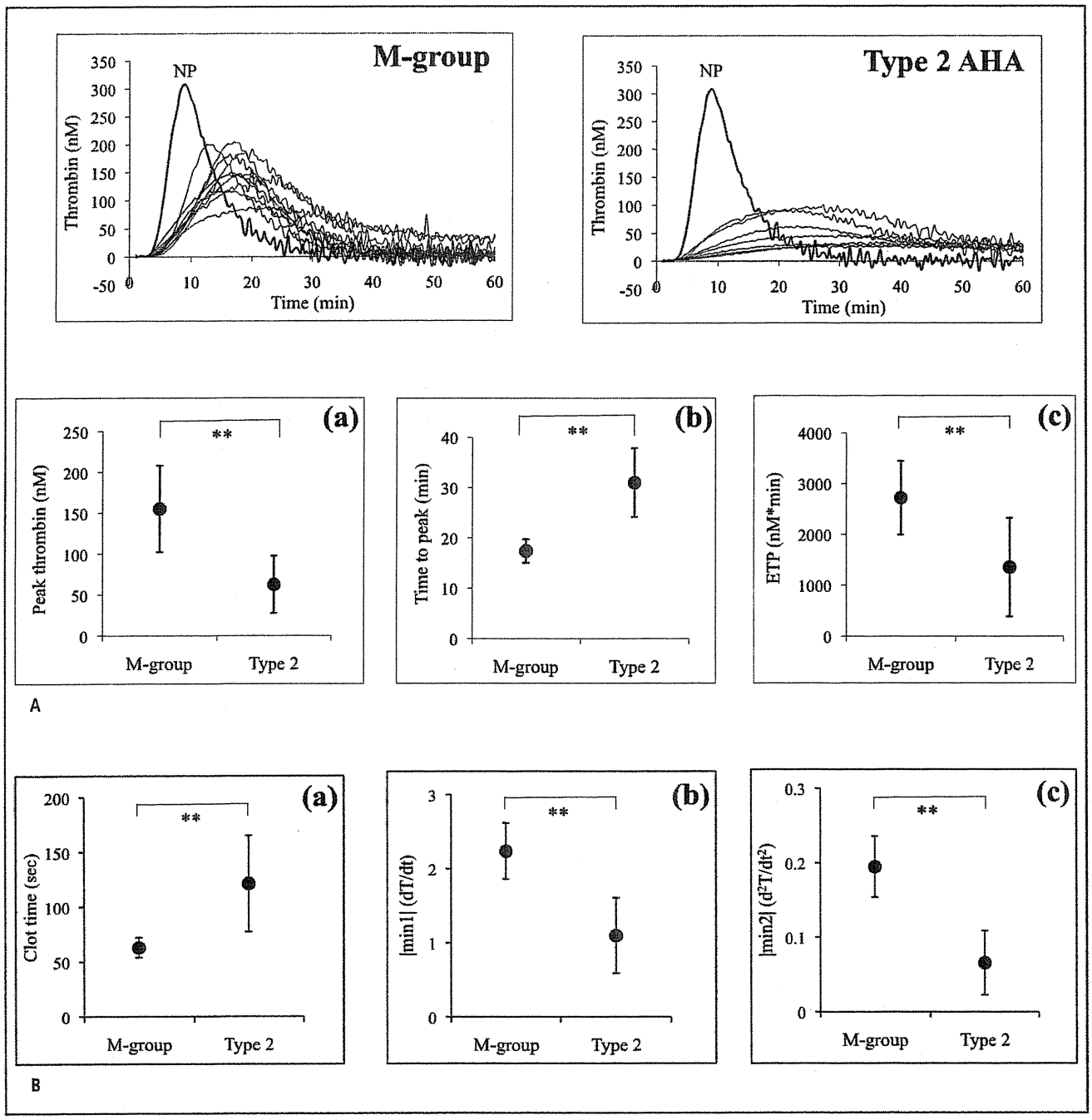

Figure 1: TGT and clot waveform analysis on patient's plasmas in the M-group and type 2 AHA. A) TGT-assay; upper panels: Plasma samples obtained from the M-group patients and type 2 AHA were preincubated with TF (0.5 pM), PL (4 μM) and ellagic acid (0.3 μM), followed by the addition of $CaCl_2$. Thrombin generation was measured as described in *Methods*, and representative TGT curves are illustrated. NP; control normal plasma. Lower panels: The peak thrombin (a), time to peak (b), and ETP (c) were derived from the TGT data obtained in upper panels. B) Clot waveform analysis; The APTT of patients' plasmas obtained from M-group and type 2 AHA were measured using the MDA-II™ system. The parameters clot time (a), |min1| (b), and |min2| (c) were derived from the clot waveform data as described in *Methods*. In all instances, results are shown as mean ± SD from at least five separate experiments. **p<0.01.

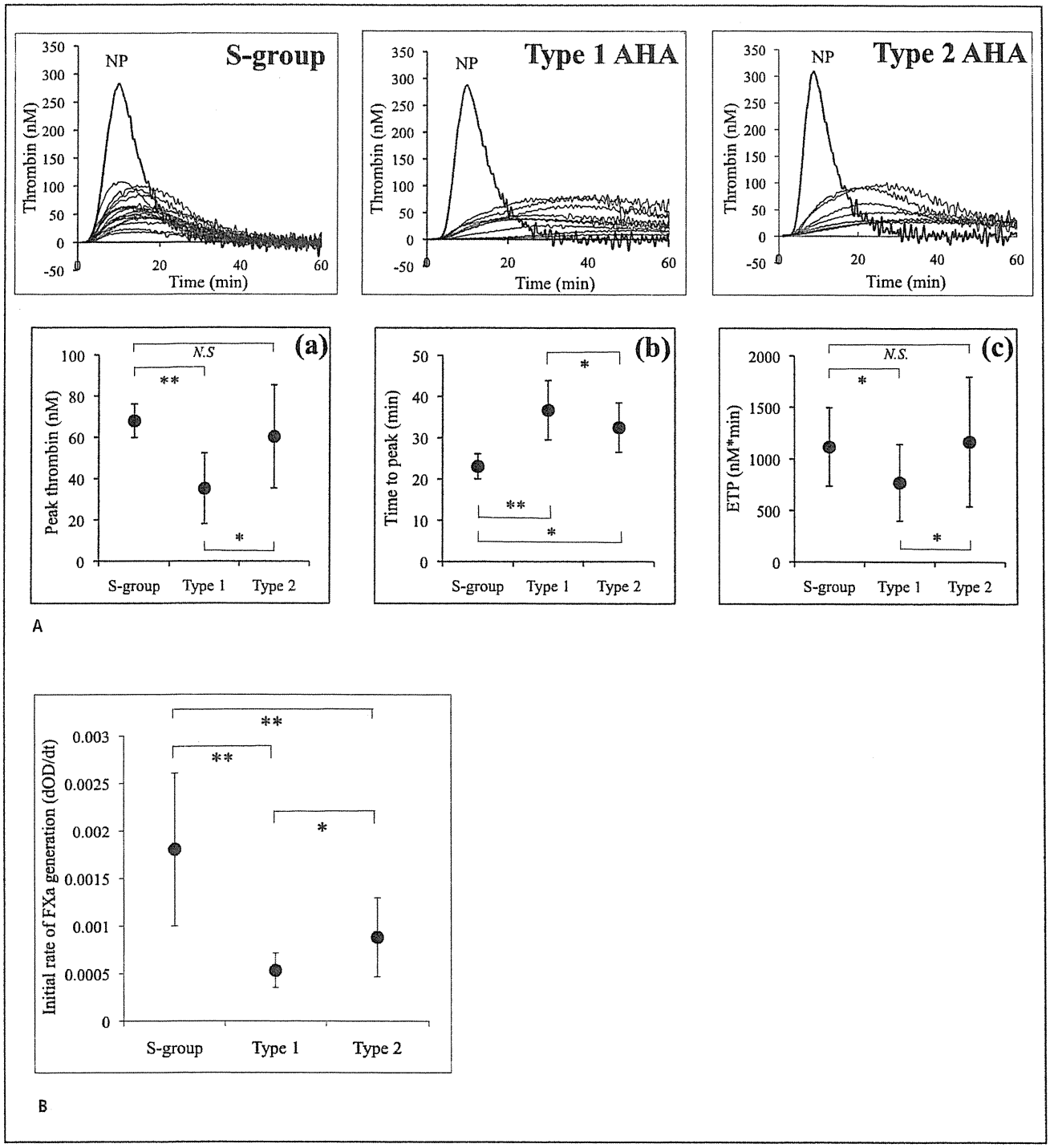

Figure 2: TGT and endogenous intrinsic FXa generation on patient's plasmas in the S-group, type 1, and type 2 AHA. A) TGT-assay; Upper panels: Patients' plasmas obtained from the S-group, type 1 AHA, and type 2 AHA were preincubated with TF (0.5 pM), PL (4 μM) and ellagic acid (0.3 μM), followed by the addition of $CaCl_2$. Thrombin generation was measured as described in *Methods*, and representative TGT curves are illustrated. NP; control normal plasma. Lower panels: The parameters of peak thrombin (a), time to peak (b), and ETP (c) were obtained from the TGT data shown in upper panels. B) Endogenous intrinsic FXa generation; Patients' plasmas obtained from S-group, type 1, and type 2 AHA were preincubated with FIXa/FX/PL mixture in the presence of hirudin, followed by the addition of $CaCl_2$ as described in *Methods*. FXa was measured using commercial reagents. The initial velocity rates of endogenous FXa generation are illustrated. In all instances, results are shown as mean ± SD from at least five separate experiments. The value of FVIII:C 1.0 IU/dl as a reference value was 5.04 ± 0.20 $x10^{-3}$. *p<0.05, **p<0.01, NS; no significance.

evaluated by clot waveform analysis using the MDA-II™ system (18). Unlike the TGT, this analysis reflects the process of fibrin formation. The data obtained from these waveforms are illustrated in ▶Figure 1B. The clot times in type 2 were prolonged by ~2.0-fold (121 ± 44/61 ± 8 seconds, p<0.05; *panel* a), compared to those in the M-group, and both |min1| and |min2| values were significantly decreased by ~2.1-fold, (1.1 ± 0.5/2.3 ± 0.3, p<0.01; *panel* b) and by ~3.1-fold (0.06 ± 0.03/0.19 ± 0.04, p<0.01; *panel* c), respectively. These results demonstrated that blood coagulation in type 2 was markedly more defective than in the M-group, despite similar FVIII:C levels (2.1 ± 0.9/2.0 ± 1.9 IU/dl, respectively). The findings were in keeping with the more severe haemorrhagic symptoms observed in type 2 relative to the M-group of patients.

Comparisons of coagulation function in severe HA (S-group) and AHA

More severe haemorrhagic symptoms are evident in the AHA patients compared to those in the S-group (FVIII:C<0.2%). These clinical differences were examined, therefore, using the TGT in these patients. Representative thrombograms from the S-group, type 1, and type 2 are illustrated in ▶Figure 2A (*upper panels*). The derived parameters are shown in the *lower panels*. The levels of peak thrombin and ETP in type 1 were markedly decreased by ~2-fold (type 1/S-group: 35.2 ± 14.1/68.0 ± 8.2 nM, p<0.01, *panel* a) and by ~1.5-fold (770 ± 310/1,115 ± 381 nM, p<0.05, *panel* c), respectively. The time to peak in type 1 was significantly prolonged by ~1.6-fold (36.7 ± 6.5/23.0 ± 3.0 min, p<0.01, *panel* b), compared to those in S-group. Similarly, in type 2, the time to peak was significantly delayed compared to that in S-group (32.5 ± 6.0/23.0 ± 3.0 min, p<0:05, *panel* b). These findings again provided strong evidence that the more serious clinical symptoms in AHA were related to the differences in global coagulation profiles, even though the FVIII:C in AHA were similar or slightly higher level than those in S-group. Surprisingly, thrombin generation in type 1 was moderately, but significantly more defective than in type 2 (p<0.05). It appeared, therefore, that coagulation function in the three groups was depressed in the order type 1, type 2, S-group.

Intrinsic FXa generation, corresponding to the upstream process of thrombin generation, was further examined to clarify the mechanism(s) of excessively defective thrombin generation in AHA. Plasma samples from each of the three groups were incubated with FIXa/FX/PL mixtures in the presence of hirudin (to eliminate thrombin reactions). $CaCl_2$ was added and endogenous intrinsic FXa generation was measured using the chromogenic assay. The initial rate of FXa generation was decreased in the order type 1, type 2, S-group (0.53 ± 0.18/0.88 ± 0.41/1.81 ± 0.78 x10^{-3}) with significant differences (▶Fig. 2B). These results were consistent with those obtained in the TGT, and further suggested that the discrepancies in coagulation function between AHA and S-group HA could be attributed to a significant decrease in the expression of intrinsic tenase complex activity (FVIIIa/FIXa/FX/PL).

Properties of anti-FVIII autoAbs in AHA

To further investigate the mechanism(s) by which the coagulation function in AHA was more defective than in the S-group, anti-FVIII autoAbs purified from AHA plasmas were characterised. FVIII levels and the basic properties of these autoAbs are summarised in ▶Table 1. Other coagulation factor activities in all cases were within the normal range (data not shown). SDS-PAGE and Western blotting using purified coagulation proteins revealed that all autoAbs reacted with FVIII alone. In particular, they all strongly reacted with the C2 domain, although some additionally reacted very faintly with the A2 domain.

The C2 domain is associated with interactions with VWF and PL (33). We examined, therefore, the effects of anti-C2 autoAbs on FVIII binding to VWF and PL in ELISA. In all type 1 cases examined the antibodies dose-dependently inhibited FVIII binding to VWF (by 64–87%) and PL (by 60–79%) at the maximum concentration of 50 μg/ml (▶Table 2), and the inhibitory effects were dose-dependent (data not shown). In contrast, in all type 2 cases the antibodies did not affect binding. Insufficient amounts of purified $F(ab')_2$ were obtained from some type 1 cases (cases 7–9) and type 2 cases (cases 16–17), however, and these individuals could not be investigated.

Different effects of anti-C2 autoAbs on thrombin-catalysed FVIII reactions

The conversion of FVIII to FVIIIa by thrombin is essential for the expression of intrinsic tenase activity (5), and one particular FVIII binding-region has been located within the C2 domain (34). We examined, therefore, the effects of anti-C2 autoAbs on thrombin-catalysed FVIII activation. FVIII (0.05 nM) was preincubated with varying amounts of AHA autoAbs. After incubation with thrombin for 1 min, the reaction was stopped by the addition of hirudin, and the reactant mixtures were diluted to completely exclude the inhibitory effects of autoAbs. FXa generation was initiated by the addition of FIXa (1 nM) and FX (150 nM) (▶Fig. 3A, *upper panel*). Results are summarised in ▶Table 2. All type 2 antibodies (50 μg/ml) decreased the peak levels of thrombin-mediated FVIII activation by 66–94%, and the inhibitory effects were dose-dependent. Type 1 autoAbs little affected these reactions (by <5%), however. In these experiments, the presence of anti-C2 autoAbs may have interfered with FXa generation and indirectly moderated thrombin-catalysed FVIII activation. To investigate this, therefore, we examined direct thrombin-catalysed FVIII cleavage in the presence of anti-C2 autoAbs. Proteolytic cleavage at Arg^{372} and Arg^{1689} is essential for generating FVIIIa activity (5). FVIII (10 nM) was preincubated with anti-C2 autoAbs (≤100 μg/ml), and was then activated by thrombin (5 nM), followed by SDS-PAGE and Western blotting using anti-A2 mAbJR8 (▶Fig. 3A, *lower panels*). All type 2 antibodies delayed the appearance of intact A2 during early-timed reactions (*panel* a). The inhibitory effects were dose-dependent by 61–73% (at 50 μg/ml), and were consistent with inhibition of

Case	Inhibition of FVIII binding to		Inhibition of thrombin-catalysed reaction of FVIII			Inhibition of FXa-catalysed reaction of FVIII			Competition of FVIII binding to	
	VWF	PL	Activation	Cleavage (%)		Activation	Cleavage (%)		ESH4	ESH8
	(%)		(%)	Arg372	Arg1689	(%)	Arg372	Arg1689	(%)	
Type 1										
1	67	72	<5	<5	<5	n.d.	n.d.	n.d.	78	12
2	86	64	<5	<5	<5	n.d.	n.d.	n.d.	69	15
3	64	60	<5	<5	<5	n.d.	n.d.	n.d.	73	<5
4	77	63	<5	<5	<5	n.d.	n.d.	n.d.	69	<5
5	72	69	<5	<5	<5	n.d.	n.d.	n.d.	63	<5
6	87	79	<5	<5	<5	n.d.	n.d.	n.d.	84	<5
Type 2										
10	<5	<5	84	70	80	68	72	>95	<5	69
11	<5	<5	81	69	72	92	66	>95	<5	77
12	<5	<5	66*	64	35	63*	72	>95	<5	64
13	<5	<5	83	61	40	95	70	>95	14	86
14	<5	<5	73	63	68	83	79	>95	19	84
15	<5	<5	94	73	80	59	54	>95	<5	67

Reactions of anti-C2 autoAbs were examined as described in *Methods*. Data represent the inhibitory effects (%) at concentrations of 50 μg/ml for all cases except for case 12* (70 μg/ml). Insufficient amounts of $F(ab')_2$ were available from cases 7–9 (Type 1) and cases 16–17 (Type 2). n.d.: not determined.

Table 2: Properties of anti-C2 autoAbs obtained from AHA patients.

cleavage at Arg^{372} (*panel* b). Similarly, inhibition of cleavage at Arg^{1689} (by 35–80%) was observed with all type 2 antibodies (▶Table 2). These cleavage patterns appeared to be little affected (by <5%) by type 1 antibodies, consistent with the results of FVIII activation.

FXa-catalysed FVIII activation was also investigated, as a target for inhibitory effect of anti-C2 autoAbs. It was difficult, however, to assess FVIIIa-dependent FXa generation in the presence of purified FXa as an activator of FVIII. Consequently, FVIII-dependent FIXa-catalysed FXa generation was evaluated. This assay depended on the positive-feedback mechanism(s) by which FIXa-catalysed FXa generation mediated FVIII activation. FVIII (0.05 nM) was preincubated with varying amounts of autoAbs, followed by the addition of FIXa (1 nM), FX (150 nM), PL (20 μM), and hirudin to initiate FXa generation (▶Fig. 3B). All type 2 antibodies (50 μg/ml) diminished the level of FXa generation by 59–95%, and the inhibitory effects were dose-dependent (*upper panel*). To directly examine FXa-catalysed FVIII proteolysis, FVIII (10 nM) was mixed with autoAbs (50 μg/ml) prior to incubation with FXa (0.5 nM) and PL (20 μM) (▶Fig. 3B, *lower panels*). All type 2 antibodies inhibited cleavage at Arg^{372} by 54–79% in a timed-dependent manner, and the inhibitory effects were dose-dependent (*panels* a and b). Cleavage at Arg^{1689} was also completely inhibited (by >95%) by all type 2 antibodies (▶Table 2). The inhibitory effects of type 1 antibodies could not be determined precisely, however, since these antibodies directly inhibited FVIII(a)-PL interaction.

Coagulation function in AHA-model reconstituted with FVIII/anti-C2 mAb

The inhibitory properties of anti-C2 type 1 and type 2 autoAbs obtained in the present study were similar to those reported by Meeks et al. (9, 10). To investigate whether the pivotal C2 epitopes of our autoAbs overlapped with those of anti-C2 mAbESH4 or mAbESH8, representing typical type 1 or type 2 behaviour, respectively, competitive inhibition for FVIII binding were examined. All type 1 autoAbs significantly competed with ESH4 binding to FVIII by 63–84%, but competed with ESH8 binding by <5–15%. In contrast, all type 2 autoAbs competed with ESH8 binding to FVIII by 64–86%, but competed with ESH4 binding by <5–19%. These findings indicated that anti-C2 type 1 and type 2 autoAbs contained the C2 epitopes identified in ESH4 and ESH8, respectively (▶Table 2).

We compared, therefore, the coagulation parameters in *in vitro* models of AHA, constructed with exogenous anti-C2 mAbs (ESH4 and ESH8), with those of the S-group. FVIII (10 IU/dl) was preincubated with ESH4 (80 μg/ml) or ESH8 (20 μg/ml), and residual FVIII:C was adjusted to <0.2 and ~2 IU/dl, respectively, similar to the levels in AHA patients. The mixtures were added to FVIII-deficient plasma and utilised in the TGT-assay (▶Fig. 4A and B). The time to peak in the AHA-models with ESH4 and ESH8 (48.8 ± 2.0/47.6 ± 2.4 min, $p<0.01/p<0.05$, respectively) were prolonged compared to the S-group (43.0 ± 1.6 min), reflecting decreased coagulation function in the presence of ESH4/ESH8. These findings

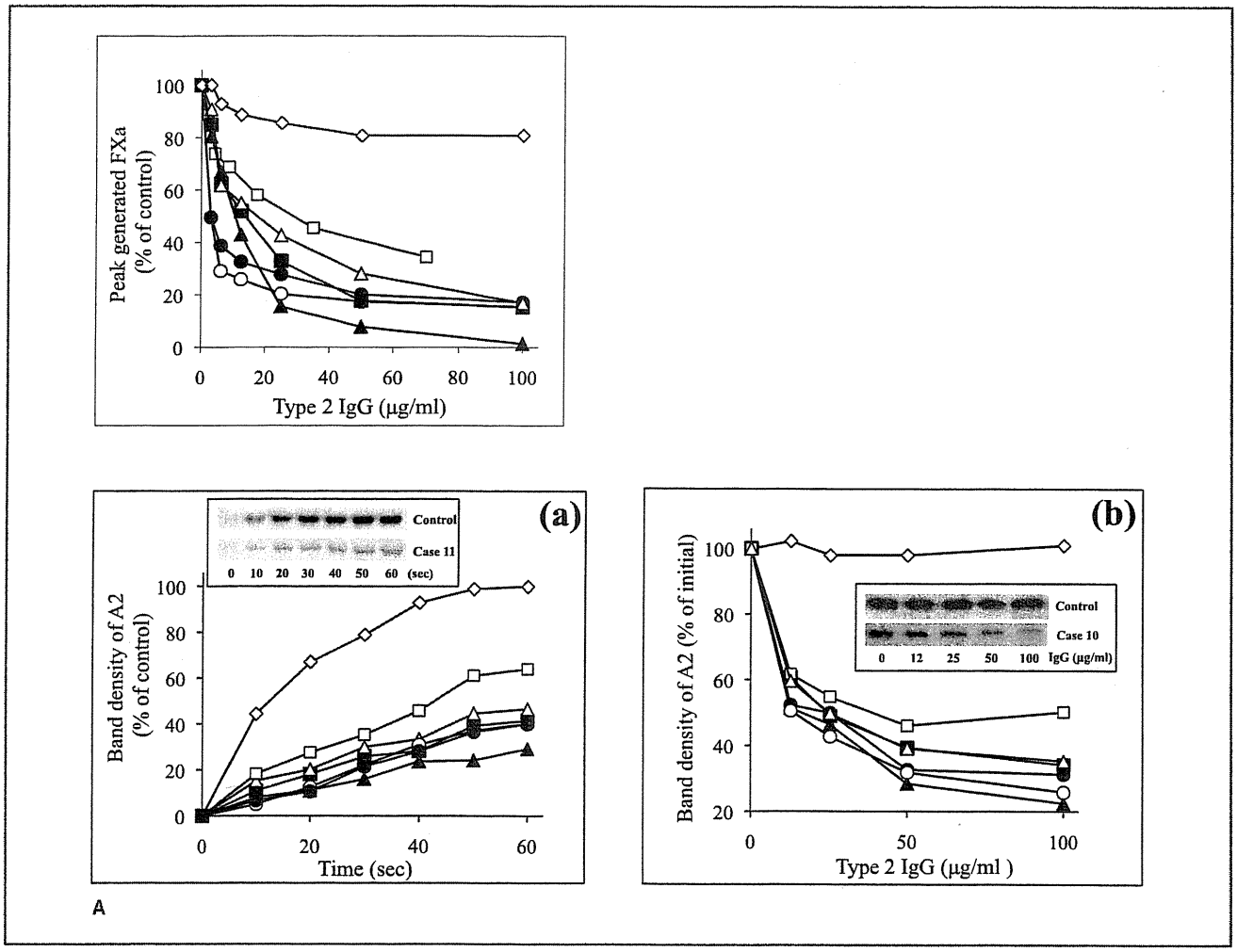

Figure 3: Effects of type 2 anti-C2 autoAbs on thrombin- or FXa-catalysed activation of FVIII. A) Thrombin reaction; Upper panel: FVIII (0.05 nM) was activated by thrombin (1 nM) for 1 min. After the addition of hirudin and dilution, FXa generation was initiated by the addition of FIXa (1 nM), FX (150 nM), and PL (20 μM). Various concentrations of type 2 autoAbs were preincubated with FVIII prior to adding thrombin, followed by adding hirudin to terminate the thrombin reaction. The rate of FXa generation without anti-C2 autoAb was regarded as 100%. In all instances, results are shown as mean from at least five separate experiments. Lower panels: (a) FVIII (10 nM) was mixed with type 2 autoAbs (100 μg/ml) for 1 h, followed by incubation with thrombin (5 nM) for the indicated times. Samples were run on 8% gel followed by Western blotting using anti-A2 mAbJR8. Band density of A2 at 1 min after adding thrombin with normal $F(ab')_2$ was regarded as 100%. (b) FVIII (10 nM) was mixed with various concentrations of type 2 autoAbs for 1 h, followed by incubation with thrombin (5 nM) for 1 min. Samples were run on 8% gel followed by Western blotting using anti-A2 mAb. Band density of A2 after adding thrombin in the absence of type 2 autoAbs was regarded as 100%. B) FXa reaction; Upper panel: FVIII (0.05 nM) was incubated with various concentrations of type 2 autoAbs for 1 h. FXa generation was initiated by the addition of FIXa (1 nM), FX (150 nM), PL (20 μM) in the presence of hirudin for 30 min. The rate of endogenous intrinsic FXa generation in the absence of autoAb was regarded as 100%. In all instances, results are shown as mean from at least five separate experiments. Lower panels: (a) FVIII (10 nM) was mixed with type 2 autoAbs (50 μg/ml) for 1 h, followed by incubation with FXa (0.5 nM) and PL (20 μM) for the indicated times. Samples were run on 8% gel followed by Western blotting using anti-A2 mAb. Band density of A2 at 5 min after FXa incubation with normal $F(ab')_2$ was regarded as 100%. (b) FVIII (10 nM) was mixed with various concentrations of type 2 autoAbs for 1 h, followed by incubation with FXa (0.5 nM) and PL (20 μM) for 5 min. Samples were run on 8% gel followed by Western blotting using anti-A2 mAb. Band density of A2 by FXa in the absence autoAbs was regarded as 100%. The symbols used are: ○; case 10, ●; case 11, □; case 12, ■; case 13, △; case 14, ▲; case 15, ◊; normal $F(ab')_2$.

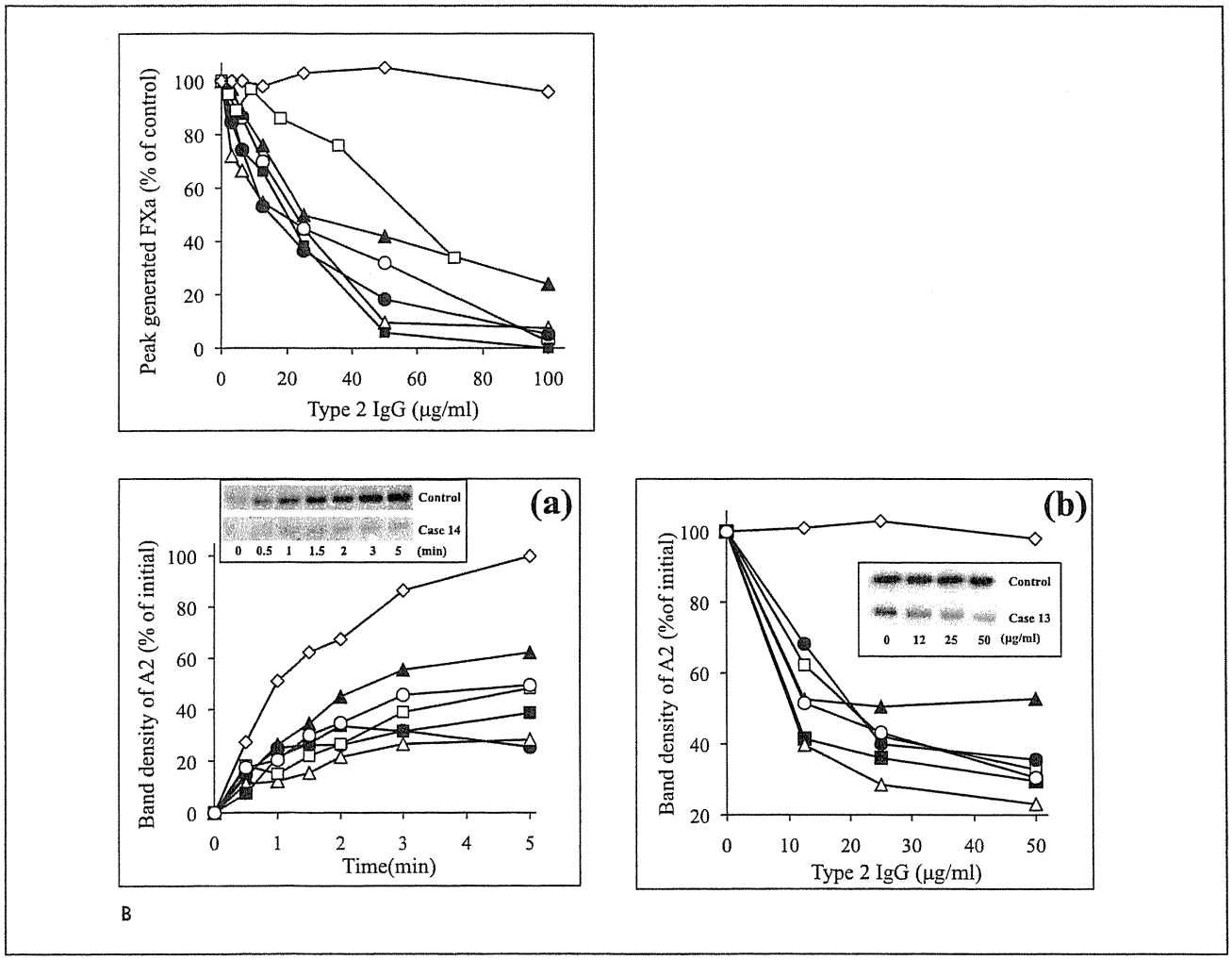

Figure 3: Continued

were in keeping with those observed using anti-C2 AHA plasmas in thrombin and FXa generation assays (see ▶Fig. 2A and B). No significant differences were observed between ESH4 and ESH8 in these assays, however.

Effect of anti-FIX mAb on TGT in FVIII-deficient plasma

Our findings suggested that the additional decrease of coagulation function in AHA relative to S-group could be attributed to the markedly decreased activity of the intrinsic tenase complex. Since intrinsic tenase activity in S-group HA depends on FIXa-catalysed FX activation, we hypothesised that inhibition of FIXa-induced FX activation could have mediated the significantly greater decrease in tenase activity observed in AHA. We examined, therefore, the effects of anti-FIX mAb on thrombin generation in FVIII-deficient plasmas (▶Fig. 5). Control experiments demonstrated that the addition of anti-FVIII alloAb (10 BU/ml) to FVIII-deficient plasmas resulted in similar TGT parameters compared to its absence, confirming complete FVIII deficiency in the plasma samples. Furthermore, the addition of anti-C2 autoAbs to FVIII-deficient plasma little affected thrombin generation (data not shown), confirming that the effects of anti-C2 autoAbs in AHA patients depended on the presence of FVIII.

In addition, anti-FIX mAb3A6 (10 BU/ml) was incubated with FVIII-deficient plasmas, and TGT assays performed as above. Peak thrombin levels in the presence of anti-FIX mAb were significantly more decreased (~1.3-fold) than its absence (8.0 ± 0.5/10.4 ± 0.6 nM, $p<0.05$, ▶Fig. A). Similarly, ETP was more depressed (~1.5-fold) in the presence of anti-FIX mAb than its absence (100 ± 10/144 ± 15 nM, $p<0.05$, ▶Fig. 5C), and the time to peak was prolonged by ~1.3-fold (32.7 ± 1.9/25.0 ± 1.8 min, $p<0.05$, ▶Fig. 5B). These findings were similar to those obtained with native AHA plasmas, and the results were consistent with the concept that the exacerbated haemorrhagic symptoms in AHA with anti-C2 autoAbs, compared to S-group, could be related, in part, to indirect

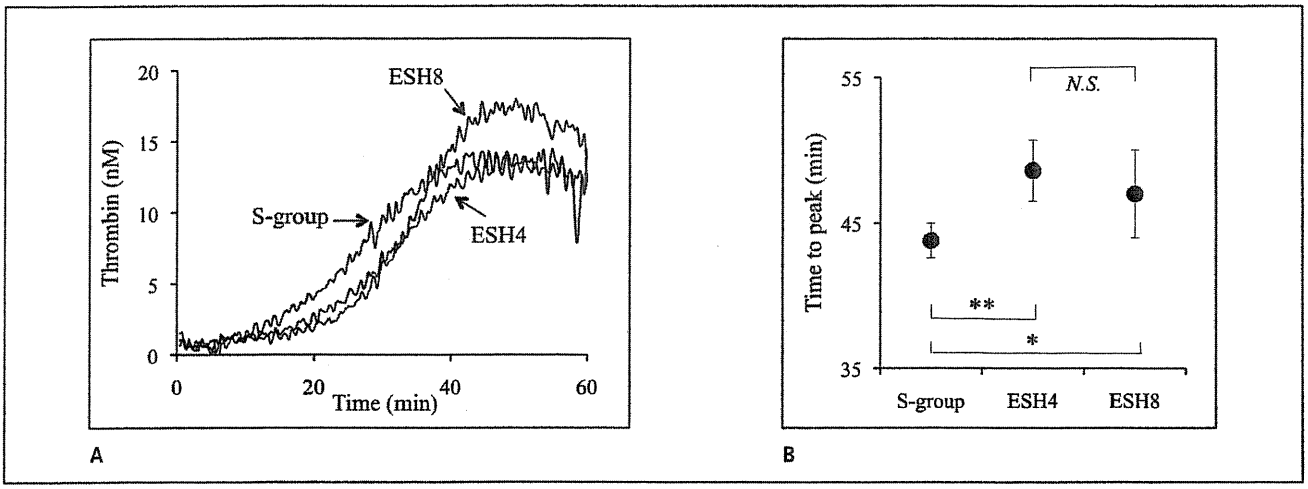

Figure 4: Coagulation function in *in vitro* AHA-models reconstituted with FVIII and anti-C2 mAb. A) FVIII (0.1 nM) was mixed with anti-C2 mAb ESH4 (80 µg/ml) or mAbESH8 (20 µg/ml) for 1 h prior to incubation with FVIII-deficient plasma. Samples were mixed with TF (0.5 pM), PL (60 µM), and ellagic acid (0.3 µM), followed by the addition of $CaCl_2$. Thrombin generation was measured as described in *Methods*. Representative TGT curves were illustrated. B) The time to peak obtained from the TGT is shown in (A). Data are shown as mean ± SD for data from at least five separate experiments. *p<0.05, **p<0.01, NS; no significance.

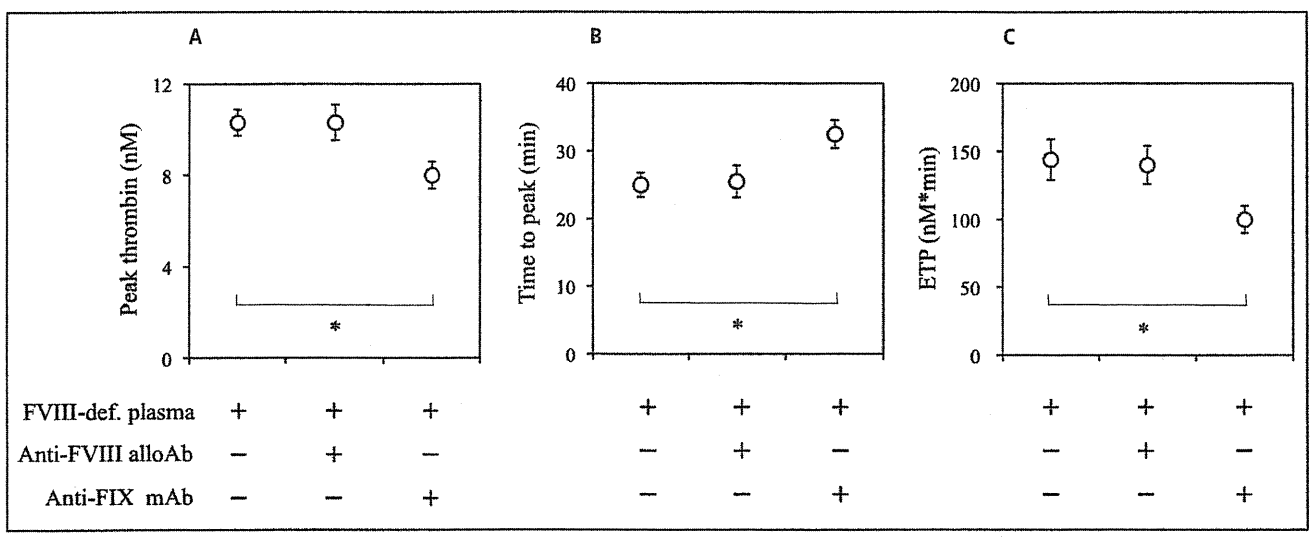

Figure 5: Effect of anti-FIX mAb on the thrombin generation in FVIII-deficient plasmas. FVIII-deficient plasma was preincubated with or without anti-C2 alloAb (10 BU/ml) for 1 h, and was reacted with or without anti-FIX Ab (10 BU/ml) for 1 h. These samples were reacted with TF (0.5 pM), PL (60 µM), and ellagic acid (1.8 µM), followed by the addition of $CaCl_2$. Thrombin generation was measured as described in *Methods*. A-C) Parameters of peak thrombin, time to peak, and ETP obtained from TGT. In all instances, results are shown as mean ± SD from at least five separate experiments. *p<0.05.

inhibition of FIXa-catalysed FX activation due to steric hindrance in the presence of the FVIII-anti-C2 autoAbs complex.

Discussion

The reason(s) why haemorrhagic symptoms in AHA are more severe than those in severe HA, although FVIII:C levels are similar, have not been clarified. The present findings suggest for the first time, that the mechanisms involved in these circumstances could possibly be attributed to the inhibition of FIXa-mediated FX activation by disturbances (steric hindrance) on the tenase complex in the presence of FVIII-anti-C2 autoAb complexes.

AHA antibodies with anti-A2 epitopes were not available for study, and all anti-FVIII autoAbs used in this study recognised the C2 domain. All anti-C2 Type 1 antibodies blocked FVIII binding to VWF and PL, but did not affect FVIII activation by thrombin. In

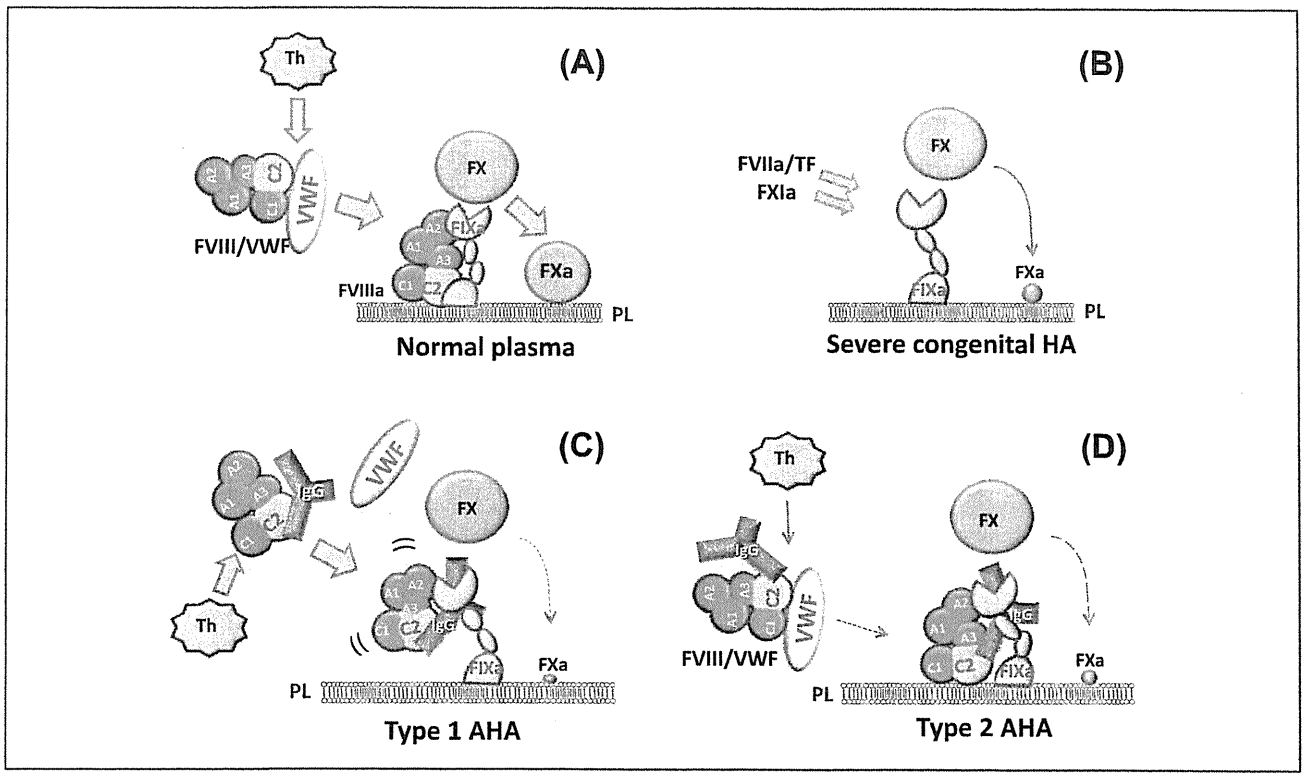

Figure 6: A putative coagulation mechanism for the intrinsic tenase complex in patients from the S-group, anti-C2 type 1, and type 2 AHA. In normal plasmas, free FVIIIa is generated from FVIII/VWF by thrombin, followed by FVIIIa/FIXa-dependent FX activation on PL micelles (A). In severe HA, FIXa alone generates FXa from FX very slowly (panel B). In both type 1 and type 2 AHA, anti-C2 IgG-FVIIIa complexes interfere with FIXa-catalysed FX activation on PL by steric hindrance. In type 1 cases, this complex fails to bind to PL, and the tenase assembly is unstable (C). In type 2 cases, although anti-C2 IgG significantly blocks thrombin-induced FVIII activation, small amounts of the FVIIIa-IgG complex bind to PL, and consequently trace amounts of tenase assembly is formed (D).

contrast, all anti-C2 type 2 antibodies inhibited FVIII activation by thrombin, but did not affect FVIII binding to VWF and PL. These anti-C2 properties were similar to those reported by Meeks et al. (9, 10), and were representative of the classical and non-classical anti-C2 antibodies respectively. In addition, PL concentrations did not affect the difference between both groups in thrombin and FXa generation and binding assays (data not shown). SDS-PAGE and Western blotting analysis revealed that the inhibition of thrombin-catalysed FVIII activation by anti-C2 Type 2 was attributed to delayed cleavage at Arg^{372} and Arg^{1689}. It was of additional interest, that mAbESH8 with type 2 epitopes did not affect FVIII cleavage by thrombin at Arg^{372} (and Arg^{1689}) (data not shown, [35]), and the findings might have reflected a novel inhibitory mechanism for anti-C2 autoAb inhibitors. The C2 domain is structurally juxtaposed to the A1 domain (36), and inhibition of cleavage by anti-C2 type 2 may have been due to a polyclonal, steric effect of the anti-C2 autoAbs, although inhibition caused by the coincident presence of an anti-A2 autoAb (37) could not be excluded. We have recently demonstrated an interaction between the C2 domain (residues 2228–2240) and the FIXa Gla domain in the tenase complex (38). In the current studies, however, neither type 1 nor type 2 anti-C2 autoAbs inhibited C2 binding to FIXa (data not shown), suggesting that these antibodies had little direct affect on FVIIIa-FIXa interactions in the tenase complex.

Thrombin generation in AHA was significantly less than that in severe HA. Furthermore, intrinsic FXa generation in AHA, reflecting processes upstream of thrombin generation, was decreased relative to that in severe HA. The anti-C2 antibodies little inhibited prothrombinase activity (data not shown), it appeared, therefore, that critical differences between AHA and severe HA in the intrinsic tenase complex contributed to the clinical findings, and that these differences centered on the effects of anti-C2 autoAbs on FVIIIa, FIXa, FX, and PL interactions. In normal tenase reactions (▶Fig. 6A), FVIII in complex with VWF, is converted to FVIIIa by thrombin and dissociated from VWF (39). FIXa (activated by FVIIa/TF and/or FXIa) together with FVIIIa, activates FX on PL-membrane surfaces, resulting in FXa generation. In severe HA in the absence of FVIIIa cofactor (▶Fig. 6B), FX is slowly converted to FXa by FIXa. Our studies demonstrated that FIXa-mediated FX activation in the presence of anti-FIX mAb, or in AHA-models constructed with anti-C2 mAbs, was less effective than that in severe HA. Based on these data, therefore, we propose a putative mechanism for the markedly decreased coagulation function in AHA with anti-C2 autoAbs. We suggest that the anti-C2 autoAbs,

complexed with FVIIIa, indirectly interfere with the association between FIXa and FX on PL-membrane surfaces by steric hindrance. Consequently, FIXa-mediated activation of FX in these patients is depressed to a greater extent than in severe HA (▶Fig. 6C and D).

The assays of thrombin and FXa generation showed that critical coagulation functions in AHA type 1 were lower than those in type 2, and experiments using AHA-models containing anti-C2 mAbs with type 1 and 2 behaviour (ESH4 and ESH8) demonstrated a similar tendency. Both native anti-C2 type 1 autoAbs and ESH4 inhibit FVIII binding to VWF and PL, and this inhibition of VWF-binding would lead to significantly decreased levels of FVIII:C (2). Furthermore, although FVIII-IgG complexes can be completely activated by thrombin, the tenase complex failed to bind to PL-membranes in these circumstances, and the conformation of this complex would likely be extremely unstable (▶Fig. 6C). In contrast, our experiments with native anti-C2 type 2 autoAbs and ESH8 demonstrated that FVIII binding to VWF or PL was little inhibited. It appeared, therefore, that these autoAbs significantly inhibited FVIII activation by thrombin, but that the relatively small amounts of FVIIIa-IgG complex formed bound to PL, facilitating trace amounts of tenase assembly (▶Fig. 6D). Nevertheless, as with type 1 antibodies, indirect disturbances (steric hindrance) mediated by FVIIIa-IgG complexes would have inhibited FIXa-induced FX activation. We speculate, therefore, that differences in the inhibitory mechanisms between type 1 and type 2 antibodies might have contributed to the observations that coagulation parameters were depressed in the order type 1, type 2, and S-group patients. Further studies are required to clarify these mechanisms.

In view of our findings that the excessive decrease in coagulation function in AHA could be due to indirect inhibition of FIXa-dependent FX activation, it might be expected that the clinical severity in patients with severe FIX-deficiency (haemophilia B, HB) might be more pronounced than in those with severe HA. In this context, it is also noteworthy that thrombin generation *in vitro* in FIXa-deficient plasmas with undetectable FIX:C (the lowest limit of detection in our laboratory is <0.2 IU/dl (18)) was significantly lower than in severe HA (unpublished observation). It is well known, however, that the clinical symptoms in severe HA are more marked than in severe HB (40, 41). The reasons for these findings remain unclear, but it may be that additional mechanism(s) underlie the AHA phenotype. For example, FX may be sequestered in a non-functional complex with FVIII-anti-C2 autoAbs in AHA. Further investigations are required to clarify these mechanisms.

The current investigations have introduced a putative mechanism for the excessive clinical haemorrhagic state in AHA, although further studies are required to support this conclusion, and to clarify the clinical differences between different types of AHA. Nevertheless, treatment of AHA in patients with high titre inhibitors has historically involved the use of coagulation-bypassing agents. Meeks et al. (9) suggested, however, that administration of high-doses of FVIII should be considered more actively for patients with AHA anti-C2 type 2 inhibitors, but not in those with type 1 inhibitors. Their conclusion was based on the findings that the activity of high-titer type 2 inhibitors could be neutralised by increasing dosages of FVIII, and it may be that in the presence of low concentrations of exogenous FVIII, anti-C2 IgGs, complexed with FVIII, indirectly disturb the association between FIXa and FX. At high doses of exogenous FVIII, inhibitory activity could be completely neutralised, and unbound (free) FVIII would be available to participate in tenase assembly. Type 1 patients failed to respond to high-dose FVIII, however, and our present data are not totally consistent with those findings. The challenging observations warrant further investigation.

What is known about this topic?

- Acquired haemophilia A (AHA) is caused by the development of factor (F)VIII autoantibodies (autoAbs).
- AHA results in more serious haemorrhagic symptoms than in congenital severe HA, but the reason(s) remain unknown, however.

What does this paper add?

- Coagulation functions, assessed using the global coagulation assays, were significantly more depressed in AHA with anti-C2 autoAbs relative to congenital HA.
- As one of putative mechanism(s), we proposed that the FVIII/anti-C2 autoAb complexes appeared to interfere with FIXa-dependent FX activation indirectly due to steric hindrance.
- In addition, the anti-C2 autoAbs with type 1 behavior prevented FVIII(a)-phospholipid binding mechanisms, essential for the tenase complex, and those with type 2 behaviour decreased the FXa generation by inhibiting thrombin-catalysed FVIII activation, suggesting that these distinct mechanisms could be associated with the exacerbated haemorrhagic symptoms in AHA.

Acknowledgement

We thank Dr. Tetsuhiro Soeda and Dr. John C. Giddings for helpful suggestions.

Conflict of interest

K.N. has received a grant from Bayer Haemophilia Award 2009.

References

1. Mann KG, Nesheim ME, Church WR, et al. Surface-dependent reactions of the vitamin K-dependent enzyme complexes. Blood 1990; 76: 1–16.
2. Hoyer LW. The factor VIII complex: structure and function. Blood 1981; 58: 1–13.
3. Wood WI, Capon DJ, Simonsen CC, et al. Expression of active human factor VIII from recombinant DNA clones. Nature 1984; 312: 330–337.
4. Eaton D, Rodriguez H, Vehar GA. Proteolytic processing of human factor VIII. Correlation of specific cleavages by thrombin, factor Xa, and activated protein C with activation and inactivation of factor VIII coagulant activity. Biochemistry 1986; 25: 505–512.
5. Fay PJ. Activation of factor VIII and mechanisms of cofactor action. Blood Rev 2004; 18: 1–15.
6. Nogami K, Shima M, Matsumoto T, et al. Mechanisms of plasmin-catalyzed inactivation of factor VIII: a crucial role for proteolytic cleavage at Arg336 responsible for plasmin-catalyzed factor VIII inactivation. J Biol Chem 2007; 282: 5287–5295.
7. Gawryl MS, Hoyer LW. Inactivation of factor VIII coagulant activity by two different types of human antibodies. Blood 1982; 60: 1103–1109.